國 立 成 功 大 學
交 通 管 理 科 學 系
博士論文

4G 通訊系統同頻干擾分析

Co-channel Interference Analysis for 4G Wireless Communication Systems

研 究 生：林郡庭
指導教授：陳文宇 博士

中華民國一百零三年七月

國立成功大學
博士論文

4G通訊系統同頻干擾分析

Co-channel Interference Analysis for 4G Wireless Communication Systems

研究生：林郡庭

本論文業經審查及口試合格特此證明

論文考試委員：陳文宇

林福林

胡大湘

指導教授：陳文宇

系(所)主管：胡大湘

中　華　民　國　103　年　7　月　26　日

摘　要

本研究分析同頻干擾對第四代無線行動通訊系統(4G)的影響，建立同頻干擾的下鏈與上鏈分析模型，並分析同頻干擾對 3GPP 長程演進技術(LTE release 10)與 IEEE 全球互通微波存取技術(IEEE 802.16m, WiMAX)的影響。

為了提高細胞邊緣用戶的傳輸速率，部分頻率重用技術常被運用在通訊系統的建置規劃中，這樣的配置方式可以有效平衡系統容量與用戶資源分配公平性間的差異。本研究在同頻干擾的下鏈分析中，將用戶採隨機均勻方式散佈於細胞覆蓋範圍內，透過計算訊號雜訊干擾比(SINR)求得平均傳輸速率，據以模擬分析並比較不同部分頻率重用方式在不同的佈建環境下，對用戶傳輸效能的影響。結果顯示本研究提出的兩種部分頻率重用方式可以有效提高細胞邊緣用戶的傳輸效能。

針對 4G 通訊系統上鏈傳輸，本研究發展評估模式以分析同頻干擾對細胞覆蓋半徑的影響。判斷上鏈通訊是否能維持的基準，是用戶在傳輸時是否具有足夠發射功率，以滿足基地台對於最低訊號雜訊干擾比的要求；距離基地台愈遠的用戶理論上需要發射的功率也愈大。模擬的結果指出同頻干擾會使細胞覆蓋範圍顯著的縮小，特別是當用戶需要更多頻譜資源以進行高速傳輸時，影響的程度更是加劇。

本研究在上鏈與下鏈的分析模式中，用戶所在地點均為隨機，對於訊號傳輸衰減模型均有考慮遮蔽的效果，另在訊號接收端均有將噪音指數納入計算。所建立的模型可以分析同頻干擾對於 LTE-A 與 IEEE 802.16m 通訊系統的影響。

關鍵字：同頻干擾、長程演進技術、全球互通微波存取、部份頻率重用、覆蓋縮減

ABSTRACT

This study analyzes the impacts of co-channel interference (CCI) on 4G wireless communication systems. Both downlink and uplink CCI analysis models are developed to estimate the influences of CCI on system performance.

To improve the throughput performance of cell-edge users, the fractional frequency reuse (FFR) technique has been commonly used in the deployment of wireless broadband networks for balancing cell capacity and user fairness. In the downlink simulation analysis, two FFR schemes are proposed to improve the performance on user and system throughput. Mobile users are randomly distributed to cell coverage, and the signal-to-interference-plus-noise ratio (SINRs) of mobile users are calculated. Average throughput is adopted to evaluate the performance of FFR schemes. The results indicate that the proposed methods can enhance edge user throughput.

In the uplink analysis, a model is developed for estimating the impacts of CCI on cell coverage. The method is based on the SINR requirement that each mobile user transmit enough power to satisfy a minimum SINR. The simulation results indicate that CCI can cause significant reduction in cell coverage, especially when the users employ more subchannels for high-speed data transmission services.

The shadow fading propagation model and user random locations are taken into consideration for both uplink and downlink analysis models. The developed model can be used to analyze CCI in Long Term Evolution and IEEE 802.16m networks.

Key words: Co-channel interference (CCI), IEEE 802.16m, LTE, fractional frequency reuse, coverage reduction

ACKNOWLEDGE

誌　　謝

博士班生涯即將邁入尾聲，心中滿滿感恩，回顧過去十年，感謝讓我蛻變的一切。這一路以來承蒙許多人的支持及鼓勵，讓我重拾信心排除困難繼續努力，終能完成博士論文，順利取得學位。

本論文之完成，首先要感謝恩師陳文字教授的悉心指導與鼓勵，在我對研究之路最徬徨時，引我進入無線通訊這個研究領域。六年以來，從修習老師的電信科技原理課程開始，到觀念架構的建立、模式設計與程式撰寫除錯，老師不斷給予提點與指導，更對論文逐字斧正，使得本論文得以順利完成，老師對學術研究嚴謹的態度與做人處事的原則亦讓我受益良多，學生將永誌於心。願老師身體健康，天天快樂開心。

在論文初審期間，承蒙本系胡大瀛博士、林珮珺博士與黃光渠博士的審閱並惠賜寶貴意見，使論文初稿內容更完整。學位口試時，交通大學電機工程系李大嵩博士、元智大學通訊工程系黃建彰博士與南台科技大學電子工程系林福林博士對論文提出許多寶貴建議與指正，謹致以最深的謝意。此外，在修業期間，本系林正章博士、張有恆博士、蔡東峻博士、呂錦山博士、陳勁甫博士對於學生在課業或生活上提供的教導與協助，在此一併致謝。

在這段日子裡。感謝碩士班學弟妹亭卉、函君、俊余、乙工、姿伶、祺真、啟瑞、馨玉、念廷、古東、忻彣、琮寶等給我的協助和陪伴，402 研究室像我在台南的另一個窩，充滿了許多回憶。感謝博士班庭煒學長在我陷入瓶頸時適時的指點、瓊文學姐與萍芬學姊對我的開示與鼓勵，同學慧華、朝祿、冠旭、子健的相互砥礪，學弟妹麗雯、繼昌、珮琪、龘祥、全志、淑秋的支持與幫助，

很高興在人生旅途當中遇見你們這群好夥伴，我會好好珍惜這個緣分。

最後，感謝支持與關心我的家人，感謝公婆願意包容我拋家棄子追求自己的目標；謝謝父母替我照顧翔翔，把他教得開朗又懂事，讓我在求學過程當中無後顧之憂；兩個弟弟桓正與桓立常替我加油打氣，很開心姐姐我終於也畢業了，你們的關懷及支持，支撐著我度過這段辛苦的日子。

感謝聖凱無條件的支持與付出，總給我正面思考與鼓勵，伴我度過低潮並轉化成奮鬥的動力，我們家的三個人，在台北，台南與越南，用電話線連成的鐵三角，雖然無形但堅韌無比。很開心在翔翔即將進入小學的時候我能回來陪他，再來希望你也能早日回台，我們在家裡等你。我明白獲得學位並不是終點，而是許多嚴峻挑戰的起點，但因為有你們，我會開心的接受，為了你們和自己努力。也因為有你們，我是幸福的，願將這份喜悅與你們分享！！

林郡庭　謹誌

2014 年 8 月於成功大學交管系

TABLE OF CONTENTS

LIST OF TABLES

LIST OF FIGURES

NOMENCLATURE

RN	Receive Node
TN	Transmit Node
IN	Interfere Node
P_{r_RN}	the received power at RN
P_{t_TN}	the transmission power of TN
L_{TN}	the path loss between TN and RN
G_{TN}	the antenna gain of TN
G_{RN}	the antenna gain of RN
I_{IN}	the interference power received at RN which radiate by IN
P_{t_IN}	the radiation power of IN
L_{IN}	the path loss between IN and RN
G_{IN}	the antenna gain of IN
$P_{t\_IN_i}$	the transmission power of IN_i
L_{IN_i}	the path loss for the link between INi to RN
G_{IN_i}	the antenna gains for IN_i
P_{r0}	the received power from BS_0 at MS_0
P_{t0}	the transmission power of BS_0
L_0	the path loss between BS_0 and MS_0
G_{BS_0}	the antenna gain of BS_0

G_{BS_1}	the antenna gain of BS_1
G_{MS_0}	the antenna gain of MS_0
G_{MS_1}	the antenna gain of MS_1
A_0	the antenna pattern of BS_0
A_1	the antenna pattern of BS_1
η_i	number of used RBs divided by the number of available RBs
P_{ti}	the transmission power of BS_i
L_i	the path loss for the link between BS_i to MS_0
G_{BS_i}	the antenna gains for BS_i
A_i	the antenna pattern of BS_i
C	the constant of propagation model
r_i	the distance between the BSi and the MSi
r_a	the distance between the interference MS to victim BS_0
μ	the path loss exponent
ε_i	the shadow fading of L_i
N_o	the white noise power
Thr_{MAX}	the maximum normalized throughput
P_t	the radiation power of MS_1
L_a	the path loss between BS_0 and MS_1
P_r	the power that BS_1 must receive
L_1	the path loss from MS_1 to BS_1
R	the cell radius
$SINR_{min}$	the minimum of require SINR for a receiver

$P_{r\_BS_0}$	the minimum reception power in BS_0
P_{TX}	the required transmission power for MS_0
P_{max}	the maximum output power of handset
P_{outage}	the service outage probability
d_{cov}	the coverage of a cell
δ	the acceptable level for outage probability
P_c	the transmission power to interior area
P_e	the transmission power to edge area
H_{BS}	the BS antenna height
H_{MS}	the MS antenna height

CHAPTER ONE: INTRODUCTION

1.1 Study Background and Motivation

In the past few years, the number of mobile phone users has rapidly increased due to the attractive design of smart phones. Mobile communication services have become deeply ingrained in people's daily lives. The development of mobile applications boosts the needs of data transmission for wireless networks. In order to enhance the transmission data rate to meet the fast growth of transmission demand, 3rd Generation Partnership Project (3GPP) proposed the Long Term Evolution (LTE) standard, and the Institute of Electrical and Electronics Engineers (IEEE) proposed the Worldwide Interoperability for Microwave Access (WiMAX) standard for broadband wireless transmission. These two systems are confirmed by International Telecommunication Union (ITU) as fourth-generation (4G) wireless communication systems for theoretical mobile transmission speed of over 100 Mbps and 1Gbps in nomadic on the downlink [1]-[7].

In general, larger spectrum resources can generate higher transmission speed and larger system capacity. But wireless spectrum resources are so rare that wireless services operators are granted only a few spectrum to provide wireless communication services to their subscribers. In this situation, aggressive frequency reuse schemes are often adopted to correct the imbalances between demand and supply of radio resources [8]. However, the aggressive reuse of spectrum reuse would cause severe inter-cell co-channel interference (CCI). The inter-cell CCI radiated from adjacent cells may degrade the transmission performance to an increasing degree as frequency reuse schemes are increasingly used in deployment of a broadband cellular network [9], [10].

Frequency reuse schemes such as reuse 1 or 3 are commonly adopted to solve the spectrum insufficient conditions. The frequency reuse schemes improve average network throughput but reduce cell-edge user throughput [11]. To improve the performance for cell-edge users, fractional frequency reuse (FFR) technique has been adopted when deploying wireless broadband networks [12]-[15].

In major 4G wireless systems such as WiMAX and LTE, orthogonal frequency division multiplexing (OFDM) technology has been adopted to improve spectral efficiency and to overcome the effect of multipath fading [16], [17]. However, OFDM is more susceptible to CCI, compared with the code division multiple accesses (CDMA) method adopted in 3G systems. Therefore, the impact of CCI on system performance should be monitored and estimated carefully when deploying a 4G cellular network. Finding ways to mitigate the CCI influence is important to help wireless services operators design their cellular network well and balance spectral efficiency and demand satisfaction at the same time.

1.2 Objectives of the Study

This study seeks to analyze the co-channel interference in 4G wireless communication networks. To do so, the research endeavors to accomplish the following objectives:

(1) To develop a CCI analysis model to describe and model the CCI of 4G communication networks.

(2) To estimate the CCI impact on system performance for 4G wireless communication networks.

(3) To explore the effect and performance of CCI mitigation schemes.

1.3 Scope of the Study

This research focuses on the two wireless communication networks: IEEE 802.16m and 3GPP LTE-Advanced (release 10). Both these two systems are confirmed as 4G wireless communication technologies by ITU. For the rest of the thesis, the term “WiMAX” means IEEE 802.16m and “LTE” means LTE release 10.

In addition, this study focuses on inter-cell co-channel interference. Because a well design directional antenna assumption, and co-channel interference power are much higher than adjacent-channel interference power, intra-cell interference and adjacent-channel interference are not addressed in this study.

This research develops a model to estimate the CCI impact on 4G communication systems. The factors that influence the communication system performance are analyzed, such as radiate power, site-to-site distance, frequency reuse, and signal modulation.

1.4 Organization of the Study

The thesis is divided into five chapters, as follows. Chapter one provides an introduction to the study, explaining the background and motivation, research objectives, scope and organization of the thesis.

Chapter two introduces two 4G wireless communication systems briefly and reviews the literature on interference analysis, interference mitigation techniques, and communication system performance analysis. The aim of this chapter is to identify how to approach analyzing the co-channel interference and evaluating the system performance in wireless communication systems.

Chapter three develops the estimate model to calculate the power of CCI. The propagation model, effect of shadow fading, user random locations, equipment radiate power, and antenna pattern are considered in the CCI estimate model.

The analysis results are presented in Chapter four. This chapter shows how much the communication system performance would decrease due to the presence of CCI. The effects of interference mitigation techniques such as power control and frequency reuse are also discussed in this chapter. Finally, the conclusions are presented in Chapter five.

CHAPTER TWO: LITERATURE REVIEW

In this chapter, we briefly present an introduction to 4G wireless communication systems. Two major subjects will be addressed, based on previous studies. The first subject is related to how the CCI happens and the solution of interference coordination or cancellation. The second subject is related to what evaluation metrics can provide an overview of the system performance.

2.1 4G Wireless Communication Systems

Multiple cell-phone technologies over generations have led to 4G wireless communication systems. The second generation (2G) brought digital technology to the industry. Multiple 2G standards were developed, but only global system for mobile communications (GSM) and IS-95A have survived. Next multiple third generation (3G) standards were developed; WCDMA by the 3GPP and CDMA2000 by Qualcomm are two widely deployed standards. To support higher transmission speed, the 3G standards were continually updated into 3.5G. WCDMA was upgraded to HSDPA, and CDMA2000 was expanded to EV-DO releases A/B. The HSPA+ upgrade from HSDPA can provide a theoretical throughput to 5.25Mbps [18].

New applications and user demand for higher throughput are pushing operators to provide higher data rates using spectrally efficient technologies. ITU is addressing these needs with International Mobile Telecommunications-Advanced (IMT-Advanced) systems.

The maximum transmission rate requirement of IMT-Advanced is 1 GB/s in low mobility and 100 Mbps in high mobility scenarios. IEEE 802.16m and LTE-Advanced (LTE-A) were submitted in October 2009 to reach the requirements for IMT-Advanced [19], [20]. The evolution of wireless standards is illustrated in Figure 2.1.

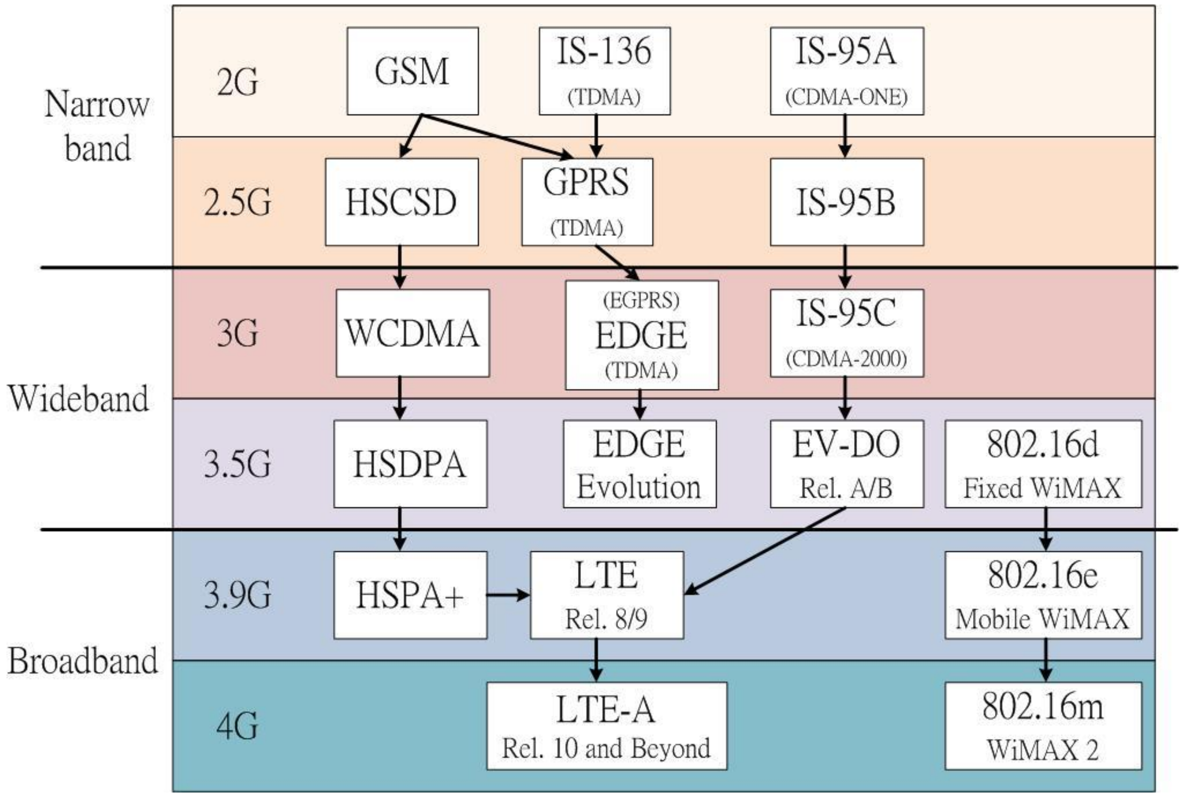

Figure 2.1 Wireless evolution – 2G to 4G

2.1.1 WiMAX

The IEEE 802.16 Working Group is a member of the IEEE 802 group for Wireless Metropolitan Area Networks, in particular Part 16: Air Interface for

Broadband Wireless Access Systems. The working group develops standards and recommended practices to support the development and deployment of fixed and mobile broadband wireless access systems. The IEEE 802.16 activities were initiated in August 1998 and the IEEE 802.16a project was approved in March 2000. The 802.16a project involved the development of a new physical layer to support enhancements to the basic data link layer.

The mobility management capabilities were added to the IEEE 802.16e project in December 2005. The IEEE 802.16 standards have evolved from line-of-sight (LOS) single-carrier fixed-wireless technology to Non-LOS (NLOS) multi-carrier mobile broadband wireless technology [21].

To fulfill the IMT-Advanced requirements, the IEEE 802.16 Working Group started the development of IEEE 802.16m in January 2007 and released the standard at the end of 2010. Building upon IEEE 802.16e mobile WiMAX, 802.16m aims for high data rate connections. IEEE 802.16m is designed as an all-IP network with a flexible MAC scheme that enables adaptation to the requirements of future internet services [20].

Orthogonal Frequency Division Multiplexing (OFDM) is adopted by the physical layer of 802.16m. OFDM is designed for the NLOS environment. It is a multicarrier modulation scheme, in which a high-rate data stream is split into several low bit-rate streams. Each substream is modulated onto a separate carrier called a subcarrier. Data are transmitted in parallel over orthogonal subcarriers. Compared to other systems, OFDM offers greater ability to address multipath fading, and it provides larger flexibility by allowing independent selection of the modulation parameters over each subcarrier [22]-[24].

In the frequency domain, an OFDM symbol consists of three types of subcarriers: the data subcarriers to transmit data, the pilot subcarriers for channel estimation, and the null subcarriers for guard bands.

Orthogonal Frequency Division Multiple Access (OFDMA) is an extension of OFDM, and it's the multiple-access technique used in 802.16m and LTE-A. In OFDMA, the available subcarriers are further divided into groups called subchannels, which can be allocated to different users. Subcarriers assigned to a subchannel need not be contiguous, letting them transmit their data in a subchannel that has better transmit condition and thus allowing for a flexible assignment of data rates to users [25]-[27].

The IEEE upgraded the 802.16e standard to 802.16m specifically for transmit speed-up. Compared to 802.16e, one of the major goals of 802.16m is the increase of data rate. By enhancing multiple input/multiple output (MIMO) antenna technology in both downlink and uplink direction and adding a multi-carrier operation, 802.16m is able to transfer more data than 802.16e in the same time period. 802.16m supports both time-division duplexing (TDD) and frequency-division duplexing (FDD). In general, TDD is the preferred duplexing method because it allows for simpler and more flexible sharing of bandwidth between uplink and bandwidth [28]. Table 2.1 provides a brief overview of the key PHY features about 802.16m and 802.16e [20].

Table 2.1 802.16 physical layer requirements

Feature	IEEE 802.16m	IEEE 802.16e
MIMO / Antenna configuration	Downlink: 2×2 (baseline), 2×4, 4×2, 4×4, 8×8, 4×8 Uplink: 1×2 (baseline), 1×4, 2×4, 4×4	Downlink: 1×1 (baseline), 1×2, 2×1, 2×2, 2×4, 4×2, 8×8, 4×8 Uplink: 1×1 (baseline), 1×2, 1×4, 2×4, 4×4
Operating bandwidth	5 to 20 MHz per carrier Carrier aggregation to achieve bandwidths up to 100 MHz	5 to 20 MHz per carrier
Frame length	Fixed frame length 5ms with Superframes (20ms), including 4 frames	Variable frame length from 2ms to 20ms, without Superframes
Duplex scheme	TDD, FDD, Hybrid FDD (MS)	TDD, FDD, Hybrid FDD (MS)

Source: [20]

2.1.2 LTE

LTE mobile communication systems are deployed as a natural evolution of GSM and universal mobile telecommunications system (UMTS). The LTE project was initiated in 2004. The motivation for deploying LTE varies, including the desire to reduce the unit cost, to use new and existing frequency bands flexible, to deploy a simplified and lower cost network with open interfaces, and to reduce in terminal complexity with an allowance for power consumption.

These high-achieving goals lead us to have more expectations for LTE, including reduced packet latency and HSPA spectral efficiency improvements of about three to four times in the downlink and two to three times in the uplink. The flexible channel bandwidths are specified at 1.4, 3, 5, 10, 15, and 20 in both the uplink and the downlink. FDD and TDD should be supported for existing paired and unpaired frequency bands, respectively. This allows LTE to be flexibly deployed in the presence of other systems [19], [29].

In the feasibility study for LTE-A, 3GPP determined that LTE-A would meet the ITU-R requirements for 4G. LTE-A is set to provide higher bitrates in a cost efficient way and focuses on higher capacity in the same time. To achieve these goals, several enhancements are being considered in LTE-A.

To achieve spectrum efficiency requirements, LTE-A aims to support downlink (8×8 antenna configuration) peak spectrum efficiency of 30 bps/Hz and uplink (4×4 antenna configuration) peak spectrum efficiency of 15 bps/Hz.

LTE-A also takes the cell-edge user into consideration. LTE-A defines the cell-edge user throughput as the 5% point of the cumulative density function (CDF) of the user throughput normalized with the overall cell bandwidth. Requirements for cell-edge performance are given below in Table 2.2.

Table 2.2 Targets for LTE-A cell edge user throughput

	Antenna configuration	**Target (bps/Hz/user)**
Uplink	1×2 / 2×4	0.04 / 0.07
Downlink	1×2 / 4×2 / 4×4	0.07 / 0.09 / 0.12

Source: [19]

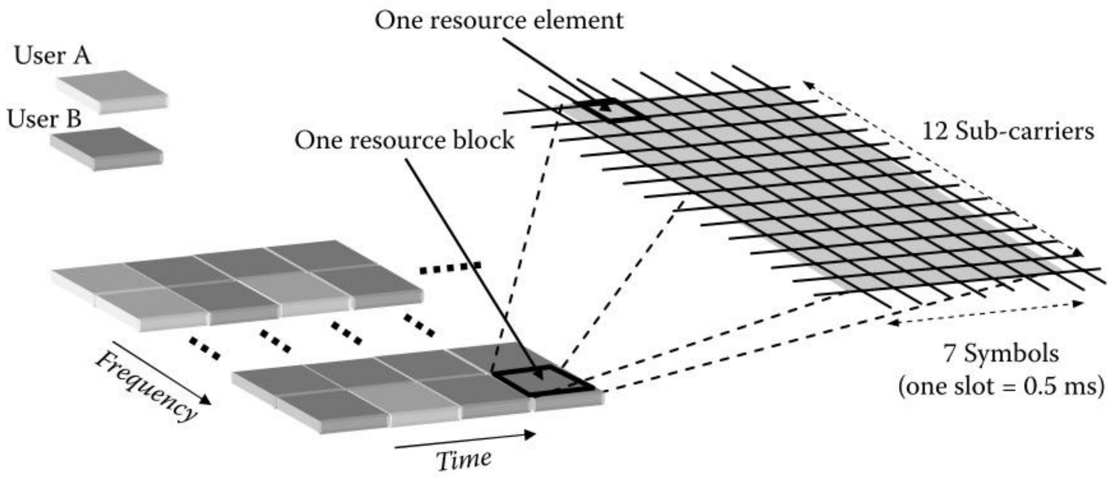

Figure 2.2 The radio resource grid of LTE

source: [30]

Figure 2.2 shows the resource grid of the uplink and downlink shared channels of LTE. The smallest unit in the resource grid is the resource element (RE), which corresponds to one subcarrier during one symbol duration. These resource elements are organized into larger blocks in time and in frequency, where seven such symbol durations constitute one slot of length 0.5 ms, and 12 subcarriers in one slot form the so-called resource block (RB). The flexible channel bandwidths and radio resources are shown in Table 2.3.

Table 2.3 The flexible radio resources of LTE

Channel bandwidth (MHz)	1.4	3	5	10	15	20
Number of resource blocks	6	15	25	50	75	100
Number of occupied subcarriers	72	180	300	600	900	1200

Source: [19]

2.2 Interference Analysis and Mitigation Technique

When a receiver receives radio signals from an unintended source, the unwanted signals are called interference. In the wireless communication systems, the interference usually happens in uplink (UL) from mobile subscribers (MS) to base station (BS), and downlink (DL) from BS to MS.

Wireless communication interference can be divided into CCI and ACI (Adjacent-Channel Interference). CCI generally refers to interference from two different radio links operating on the same frequency channel. The receiver will receive the wanted signal and harmful interfering signal at the same time.

ACI is interference caused by extraneous power from a signal in an adjacent channel. It happens when adjacent channels do not keep enough channel space or have inadequate filtering so that the signals in adjacent channels interfering with each other.

The ACI that receiver A receives from transmitter B is the power summary that B emits into A’s channel. This unwanted emission is represented by the Adjacent Channel Leakage Ratio (ACLR). The power that A picks up from B's channel is represented by the Adjacent Channel Selectivity (ACS). These two interferences will happen both at BS or MS [31].

2.2.1 Interference Analysis

A number of previous studies have been conducted on interference in communication systems. In [32], the author calculated the signal-to-interference ratio (S/I) under different system parameters such as cluster size, filter characteristics, propagation exponent, tier coverage and directional antennae front-to-back ratio in cellular communications systems. The author proved that the CCI and ACI cannot be ignored because they may create severe performance degradation in some operating environments.

In [33], the author studied the impacts of ACI on uplink capacity in a multi-macrocell/multi-microcell wideband code-division multiple access (WCDMA) system. To describe the ACI impact, the author randomly distributed the mobile users and accounts shadow fading in uplink interference analysis. The results indicated that both the base station separation and adjacent channel interference power ratio (ACIR) affect system capacity reduction.

In [8], the authors analyzed the reduction in cell coverage caused by CCI in an IEEE 802.16m system. The analysis model was based on the SINRs requirement in which each BS must receive enough power to maintain a minimum SINR for their mobile users. The results showed that CCI can cause significant reduction in cell coverage, especially when mobile users need a large amount of spectrum resources for high speed data transmissions.

2.2.2 Inter-cell Interference Coordination

Aggressive frequency reuse schemes due to scant spectrum resources lead to the wireless communication systems suffering from inter-cell co-channel interferences. An interference-limited system cannot achieve the full potential capacity that the 4G standard can support without the implementation at the BS and MS of one or more viable interference mitigation techniques [11]. There are two major solutions of inter-cell interference coordination (ICIC) techniques: power control and fractional frequency reuse (FFR).

2.2.2.1 Power Control

The main goal of power control in wireless communication systems is limiting or controlling inter-cell interference, in particular for cell edge users. In [34], the authors proposed an analytical approach for the study of fractional power control compensation factor in LTE networks. The research outcomes showed that the optimal compensation factor is highly dependent on the path-loss coefficient. Fractional power control can also lead to huge gains of cell spectral efficiency over full compensation power control.

In [35], uplink fractional power control in LTE was analyzed. They found that there are trade-off between cell edge bitrate and cell capacity. Compared to the traditional full compensation open or closed loop, fractional power control improved the cell-edge bitrate, average bitrate, and system capacity up to 20% and reduced the power consumption at the same time.

2.2.2.2 Fractional Frequency Reuse

In wireless communication networks, co-channel interference is mainly caused by frequency reuse. Since a large amount of spectrum is hard to come by, aggressive frequency reuse is required for the deployment of a broadband cellular network [8]. Frequency reuse means that spectrum allocated for the system is reused multiple times. The ratio of carrier to interference powers(C/I) will decrease at the periphery of cells if the co-channel interference is not minimized. The lower C/I causes diminished system capacity, more frequency handoffs and dropped calls. It is demonstrated in [11] that the most aggressive frequency reuse pattern (reuse factor=1) improves average network throughput but reduces cell-edge user throughput because of severe CCI.

To improve the performance of cell-edge users, the fractional frequency reuse (FFR) technique has been adopted in the deployment of wireless broadband networks [12]-[15]. The FFR scheme usually partitions a cell into two geographical regions: the interior area and the edge area [14]. The basic idea of this scheme is to employ a small frequency reuse factor (i.e. reuse factor=1) for cell-interior users who, in general, have high SINRs and to use a large frequency reuse factor (i.e. reuse factor=3) for cell-edge users. The FFR schemes also divide the whole frequency band into several sub-bands that would be assigned to different regions. FFR can be used in uplink or downlink transmissions, but is generally adopted in the downlink [15].

2.3 System Performance Analysis

The research reported in [36] examined the impact of CCI and ACI on system capacity in cellular radio systems. The CCI and ACI influence the transmission bit error rate (BER), and there exists a trade-off between system capacity and BER. The authors' simulation results showed that CCI is more harmful than ACI in some situations. When the channel spacing is greater than or equal to signal bandwidth, the ACI will decrease to zero, but the CCI is still present because of channel reuse.

In [37], the authors investigated the performance of FFR schemes by throughput. The average cell throughputs can be calculated from SINR. The cell average throughput changes when given different interior region radius. The optimal distance threshold can identify the cell-center and cell-edge users for FFR schemes.

In [38], the author performed analysis to find the optimal FFR in multicellular OFDMA system. The cell throughput and the interior region radius for various FFR factors of the exterior region were calculated to evaluate the effects of FFR factor. Results showed that the optimal interior region radius is 0.63Km when the cell radius is 1Km, and that the optimal frequency reuse factor of the exterior region is 3.

According to the previous studies about wireless communication systems, we will present cell coverage, the user SINR, and network throughput as our system performance evaluation metrics, with the interior region radius in FFR schemes set as 0.6.

CHAPTER THREE: SYSTEM MODEL

In this chapter, the analysis model of CCI in wireless communication networks will be developed.

3.1 Co-channel Interference Power

Consider the co-channel signal transmissions in a cellular system, as shown in Figure 3.1. We first examine the CCI power from one of the adjacent cells. For any given receive node (RN), it receives both the desired signal from the transmit node (TN) in the communication link and CCI signals from the interfere node (IN) that uses the same frequency channel in adjacent cells.

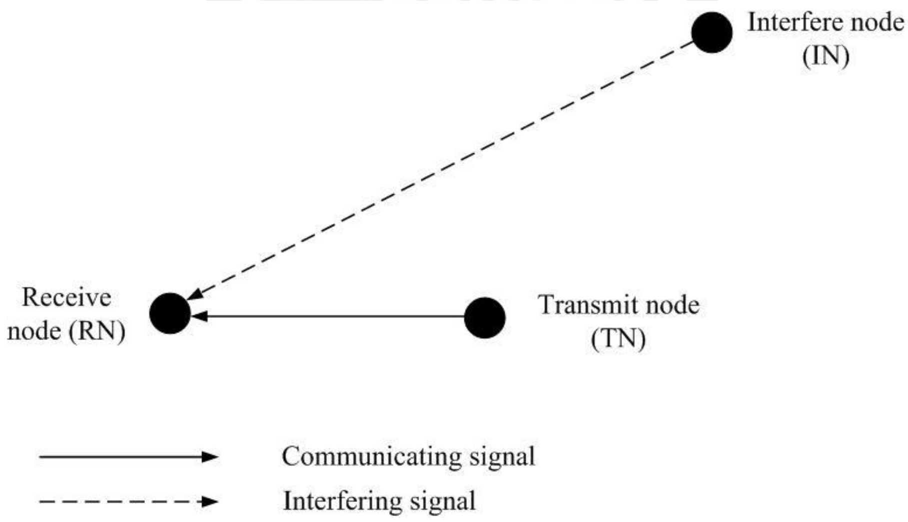

Figure 3.1 CCI from one of the interfere nodes in an adjacent area

In this situation, the received power P_{r_RN} at RN from TN can be expressed as

$$P_{r\_RN} = P_{t\_TN} \cdot L_{TN} \cdot G_{TN} \cdot G_{RN} \tag{3-1}$$

where P_{t_TN} is the transmission power of TN; L_{TN} is the path loss between TN and RN; and G_{TN} and G_{RN} are the antenna gain of TN and RN, respectively.

On the other hand, the interference power I_{IN} received at RN from IN is given by

$$I_{IN} = P_{t\_IN} \cdot L_{IN} \cdot G_{IN} \cdot G_{RN} \tag{3-2}$$

where P_{t_IN} is the radiation power of IN; L_{IN} is the path loss between IN and RN; and G_{IN} is the antenna gain of IN.

Assume there are k INs in the network. The total co-channel interference power received at RN can be calculated as

$$CCI_{total} = \sum_{i=1}^{k} P_{t\_IN_i} \cdot L_{IN_i} \cdot G_{IN_i} \cdot G_{RN} \tag{3-3}$$

where $P_{t\_IN_i}$ is the transmission power of IN_i; L_{IN_i} is the path loss for the link between IN_i and RN; and G_{IN_i} is the antenna gain for IN_i.

3.2 Antenna Radiation Pattern

The basic BS structure in this research is presented as Figure 3.2. The base station is deployed in the center of three hexagon sectors: S_1, S_2, and S_3. The BS radiates to each sector by directional antennas. The interference analysis model in this research will take the BS antenna pattern into consideration.

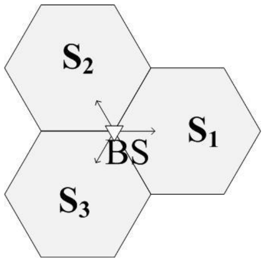

Figure 3.2 One BS structure

The BS antenna pattern $A(\theta)$ used in the simulation in each sector in three-sector cells is specified in [39], [40] as

$$A(\theta)_{(dB)} = -\min\left[12\left(\frac{\theta}{\theta_{3dB}}\right)^2, A_m\right], \quad -180^\circ \le \theta \le 180^\circ \tag{3-4}$$

where θ_{3dB} is the 3dB beam width (which corresponds to 70 degrees in IEEE 802.16m and 65 degrees in LTE-A) and A_m = 20 dB is the maximum attenuation from -180° to 180°. The antenna pattern is shown in Figure 3.3. The BS antenna gain is assumed to be 15 dBi. For mobile station antennas, an omni-directional radiation pattern with a gain of 0 dBi is assumed.

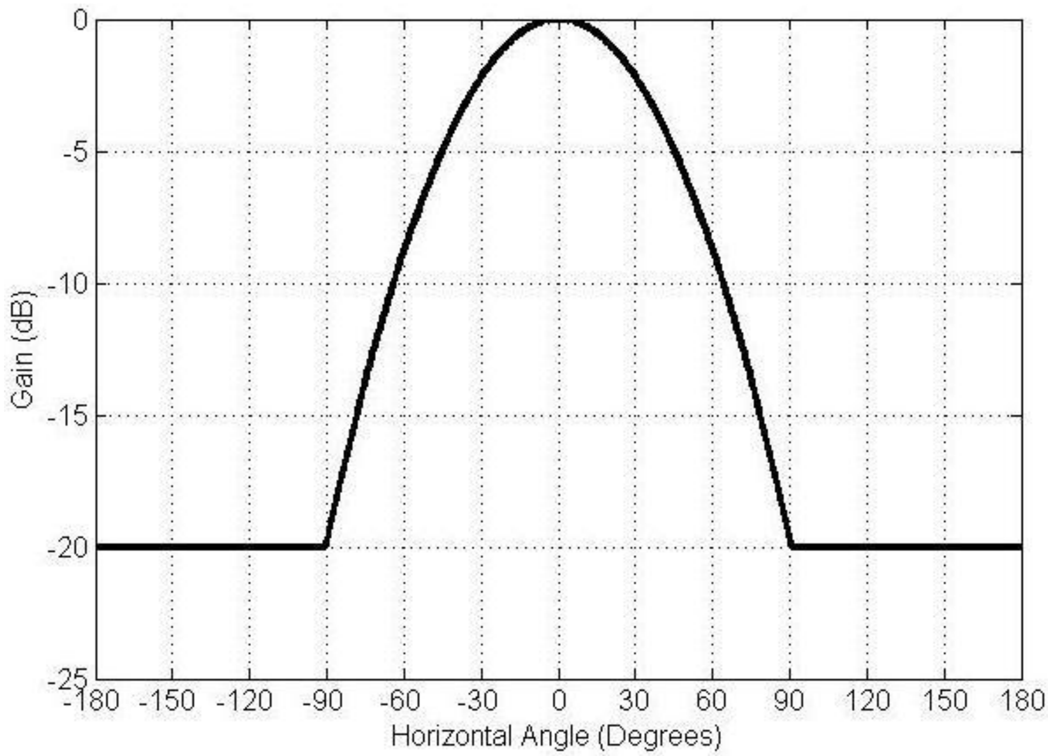

Figure 3.3 Antenna pattern for base station.

3.3 The Downlink Co-channel Interference Analysis Model

Consider downlink transmissions in a cellular system, as shown in Figure 3.4. Any given mobile station receives both the desired signal from its serving BS and CCI signals from adjacent BSs.

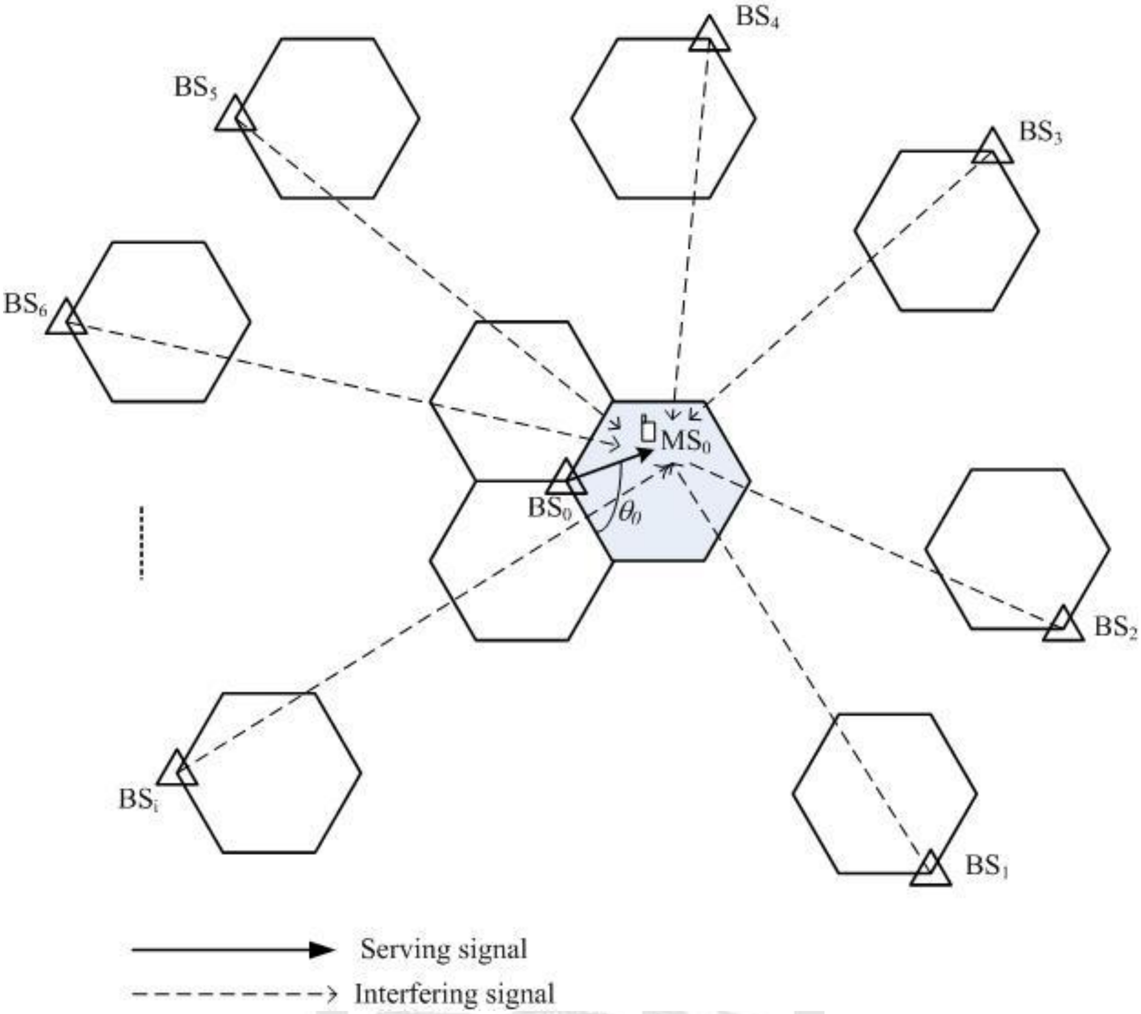

Figure 3.4 Downlink CCI from adjacent cells.

Taking the antenna pattern effects into consideration, the received power from BS_0 at MS_0 can be extended from (3-1) as

$$P_{r0} = P_{t0} \cdot L_0 \cdot G_{BS_0} \cdot G_{MS_0} \cdot A_0(\theta_0 - 60°), \tag{3-5}$$

where P_{t0} is the transmission power of BS_0; L_0 is the path loss between BS_0 and MS_0; G_{BS_0} and G_{MS_0} are the antenna gain of BS_0 and MS_0, respectively; θ_0 is the included angle of MS_0 and BS_0 cell sideline, and A_0 is the antenna pattern of BS_0, and the θ_0 should be minus 60° to fit the definition about θ in (3-4). Note that the pattern of MSs is assumed to be omni-directional.

This analysis model attempts to calculate the maximum capacity that a BS can provide in the presence of inter-cell CCI. Assume the reference site (BS_0) is operated in fully loaded condition, in which all the available resource blocks (RBs) are used. Each MS obtains just one RB and could receive interference signals coming from adjacent BSs. Figure 3.4 shows how the victim mobile station MS_0 experiences downlink CCI from the adjacent BSs.

Assume there are k interfering BSs in our model. Given BS_i, the traffic load η_i is defined by the number of used RBs divided by the number of available RBs. The total interference power received at MS_0 can be calculated as

$$CCI_{total} = \sum_{i=1}^{k} \eta_i \cdot P_{ti} \cdot L_i \cdot G_{BS_i} \cdot G_{MS_0} \cdot A_i(\theta_i - 60^{\circ}) \tag{3-6}$$

where P_{ti} is the transmission power of BS_i, L_i is the path loss for the link between BS_i and MS_0, G_{BS_i} is the antenna gain for BS_i, θ_i is the included angle of MS_0 and BS_i cell sideline, and A_i is the antenna pattern of BS_i.

Taking the shadow fading effect into account, the propagation model can be modeled as

$$L_i = C \cdot r_i^{-\mu} \cdot 10^{\varepsilon_i/10}, \tag{3-7}$$

where C is a constant, r_i is the distance between the BS and the MS, and μ is the path loss exponent; ε_i, which represents the shadow fading effect, in general is a Gaussian random variable with zero mean and standard deviation σ [41].

In the analysis of wireless communication network performance, the baseline throughput primarily depends on the SINR values of a communication link. In the downlink analysis that takes the MS receiver noise-figure (NF) into account, the *SINR* received at the victim MS is

$$SINR_0 = \frac{P_{t0} \cdot L_0 \cdot G_{BS_0} \cdot G_{MS_0} \cdot A_0(\theta_0 - 60°)}{(NF_{MS} \cdot N_0) + \sum_{i=1}^{k} \eta_i \cdot P_{ti} \cdot L_i \cdot G_{BS_i} \cdot G_{MS_0} \cdot A_i(\theta_i - 60°)}, \qquad (3\text{-}8)$$

where N_o is the white noise power. Given n RBs, the noise power in dB scale can be calculated by

$$N_{o\,(\mathrm{dB})} = -174 \text{ dBm/Hz} + 10\log_{10}(n \times BW_{\mathrm{rb}}), \qquad (3\text{-}9)$$

where BW_{rb} is the bandwidth of a resource block.

Using the link adaptation model specified in [40], the normalized throughput over a channel with a given SINR can be given by

$$Thr = \begin{cases} 0 & \text{for SINR} < SINR_{MIN} \\ \alpha \cdot \log_2(1 + \text{SINR}) & \text{for } SINR_{MIN} < \text{SINR} < SINR_{MAX} \\ Thr_{MAX} & \text{for SINR} > SINR_{MAX} \end{cases} \qquad (3\text{-}10)$$

where $\log_2(1+\text{SINR})$ is the Shannon bound representing the maximum theoretical throughput; α is the attenuation factor; and Thr_{MAX} is the maximum normalized throughput, which is equal to 4.4 bps/Hz in this study. For downlink transmission, α is set to 0.6. The $SINR_{NIN}$(dB) is about -15 dB where the throughput value approach to 0 and the $SINR_{MAX}$(dB) is about 22.05 when the throughput is 4.4. The relationship between normalized throughput and SINR(dB) is shown in Figure 3.5.

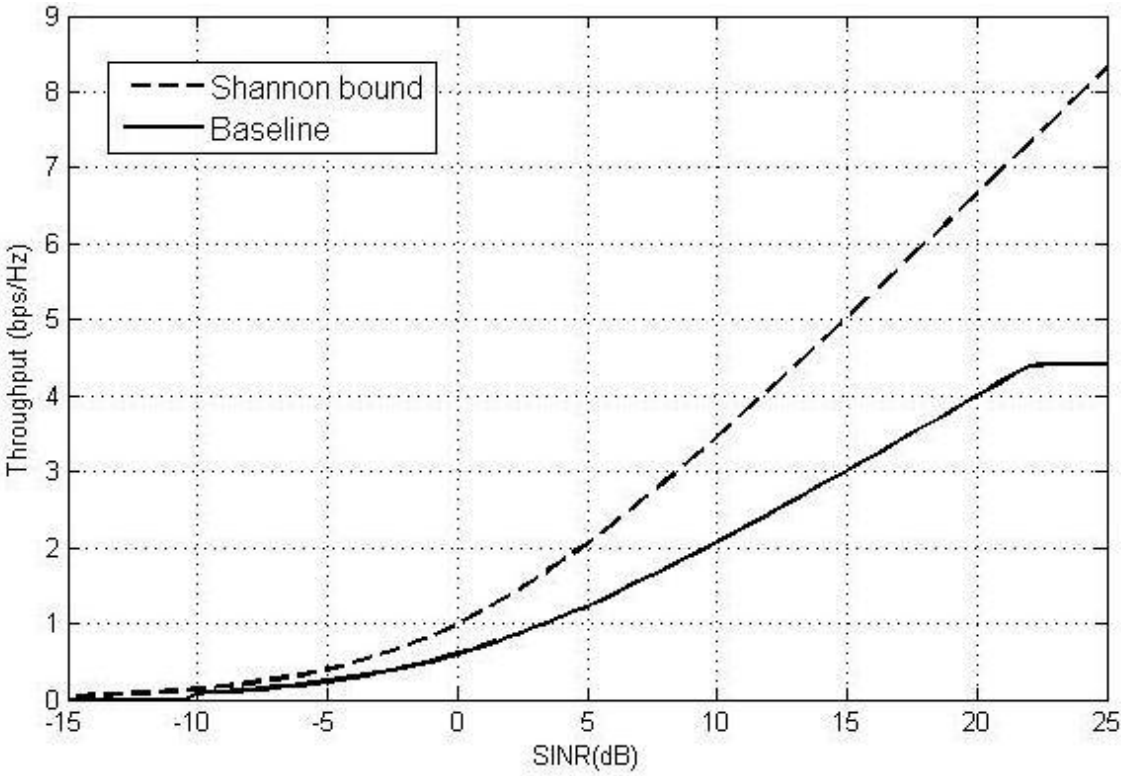

Figure 3.5 Baseline throughput for adaptive modulation scheme.

3.4 The Uplink Co-channel Interference Analysis Model

In studying the uplink CCI analysis model, we first examine the average CCI power from one of the adjacent cells. As shown in Figure 3.6, two mobile users MS_0 and MS_1 communicate with BS_0 and BS_1, respectively. Assume they use the same frequency channel. In this situation, the communication link between MS_0 and BS_0 will suffer from uplink CCI because BS_0 can receive the co-channel signal radiated from MS_1. Based on Figure 3.6 and the reference [8], we can build the uplink CCI analysis model.

The interference power received at BS_0 from MS_1 is given by

$$I_1 = P_t \cdot L_a \cdot G_{MS_1} \cdot G_{BS_0} \cdot A_0(\theta_a - 60°), \tag{3-11}$$

where P_t is the radiation power of MS_1; L_a is the path loss between BS_0 and MS_1; G_{MS_1} and G_{BS_0} are the antenna gain of MS_1 and BS_0, respectively; and A_0 represents the antenna pattern of BS_0.

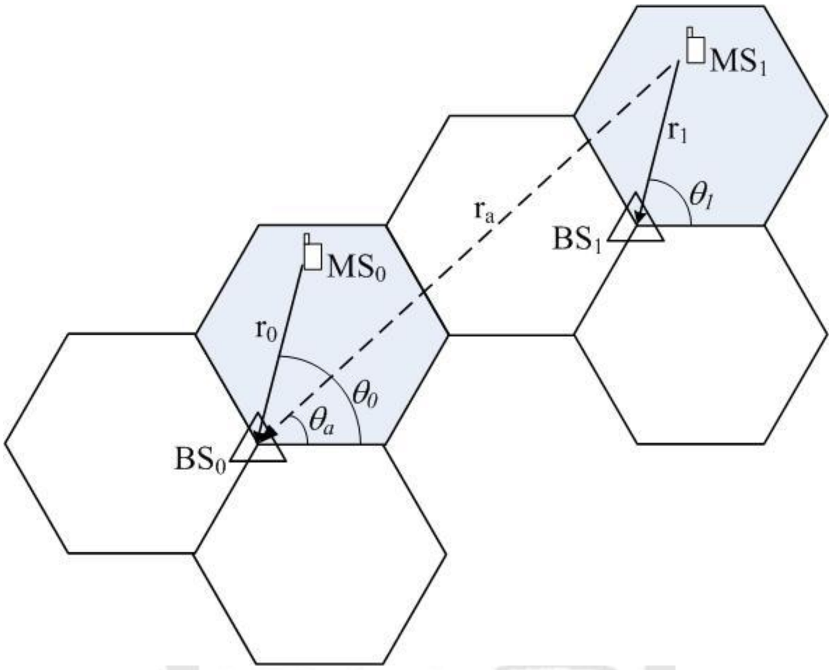

Figure 3.6 Uplink CCI from one of the adjacent cells.

Also, MS_1 must provide sufficient power for the communication link between MS_1 and BS_1. In other words, P_t is determined by the power P_r that BS_1 must receive. That is,

$$P_r = P_t \cdot L_1 \cdot G_{MS_1} \cdot G_{BS_1} \cdot A_1(\theta_1 - 60°), \tag{3-12}$$

where L_1 is the path loss from MS_1 to BS_1, G_{BS_1} is the antenna gain of BS_1, and A_1 represents the antenna pattern of BS_1.

Assume the two BSs have the same antenna gain. Substituting (3-12) into (3-11), we can obtain

$$I_1 = P_r \cdot \frac{L_a}{L_1} \cdot \frac{A_0(\theta_a - 60°)}{A_1(\theta_1 - 60°)} \tag{3-13}$$

Taking the shadow fading effect into account, the path loss from MS_1 to BS_0, similar to (3-7), can be expressed as

$$L_a = C_a \cdot r_a^{-\mu_a} \cdot 10^{\varepsilon_a/10}, \tag{3-14}$$

where C_a is a constant, μ_a is the path loss exponent, and ε_a represents the shadow fading effect.

Similarly, the path loss from MS_1 to BS_1 is given by

$$L_1 = C_1 \cdot r_1^{-\mu_1} \cdot 10^{\varepsilon_1/10} \tag{3-15}$$

For simplification, assume $C_a=C_1=C$, $\mu_a=\mu_1=\mu$, and ε_a and ε_1 are two identical and independent random variables. The shadow fading can be modeled as a random variable with lognormal distribution in the mobile communication environment. From equations (3-13)-(3-15), we can observe that the power level of I_1 depends primarily on the random location of MS_1 and the two fading effects. Assume the mobile user's random location and the random variables of shadow fading are independent. The expected value of I_1 is given by [33]:

$$E(I_1) = Pr \cdot E\left[10^{(\varepsilon_a - \varepsilon_1)/10}\right] \cdot E\left[\left(\frac{r_1}{r_a}\right)^{\mu} \cdot \frac{A_0(\theta_a - 60°)}{A_1(\theta_1 - 60°)}\right] \tag{3-16}$$

Further, since ε_a and ε_1 are two identical and independent random variables with lognormal distribution, their difference is still a lognormal random variable with zero mean and variance $2\sigma^2$. Hence we can obtain

$$E\left[10^{(\varepsilon_a-\varepsilon_1)/10}\right]=e^{\sigma^2(0.1\cdot\ln 10)^2} \tag{3-17}$$

The random location effect of the interfering source on the interference power can be modeled by integration over the sector area where mobile user MS_1 is located. Therefore, the expected value of I_1 can be rewritten as

$$E(I_1)=Pr\cdot e^{\sigma^2(0.1\cdot\ln 10)^2}\cdot\int_0^R\int_0^{\frac{2\pi}{3}}\left(\frac{r_1}{r_a}\right)^{\mu}\cdot\frac{A_0(\theta_a-60°)}{A_1(\theta_1-60°)}\cdot f(r_1,\theta_1)d\theta_1 dr_1, \tag{3-18}$$

where R is the radius of BS_1. Note that $f(r_1,\theta_1)$ is the probability density function for the random location of MS_1. If the random location is uniformly distributed over the 120° sector, the probability density function is

$$\begin{aligned} f(r_1,\theta_1) &= f(r_1)\cdot f(\theta_1) \\ &= \frac{2r_1}{R^2}\cdot\frac{3}{2\pi}=\frac{3r_1}{\pi R^2}, \qquad 0<r_1<R,\ 0<\theta_1<\frac{2\pi}{3} \end{aligned} \tag{3-19}$$

To calculate the interference power at BS_0, we also need to determine the power P_r that BS_1 must receive. In practice, a minimum of SINR is required for a receiver to demodulate signals into a bit stream. Also, taking receiver's noise figure (NF) into consideration, from [26], we have

$$P_r = SINR_{\min}\cdot NF\cdot N_0, \tag{3-20}$$

where N_0 is the white noise power. Given n subchannels, the noise power can be calculated by (3-9).

If there are k interfering cells, the total interference power received at BS_0 is given by

$$CCI_{total} = \sum_{j=1}^{k} E[I_j] \tag{3-21}$$

Next, the CCI impact on system performance, which accounts for the handset output power limitation, is analyzed. When the interference signals are present at the victim BS_0, its minimum reception power can be expressed as

$$P_{r\_BS_0} = SINR_{\min} \cdot (NF \cdot N_0 + CCI_{total}) \cdot \tag{3-22}$$

Then, we need to examine whether MS_0 has enough transmission power to support the above power requirement. The required transmission power for MS_0, denoted by P_{TX}, must satisfy the following power link budget

$$P_{r\_BS_0} = P_{TX} \cdot C \cdot r_0^{-\mu} \cdot 10^{\varepsilon_0/10} \cdot G_{MS_0} \cdot G_{BS_0} \cdot A_0(\theta_0 - 60°). \tag{3-23}$$

Equation (3-23) can be rewritten as

$$P_{TX} = \frac{P_{r\_BS_0}}{C \cdot r_0^{-\mu} \cdot 10^{\varepsilon_0/10} \cdot G_{MS_0} \cdot G_{BS_0} \cdot A_0(\theta_0 - 60°)} \tag{3-24}$$

Because each handset has a constraint on output power, the communication service is not available when the required transmission power is greater than the handset's maximum output power. Therefore, the service outage probability is given as

$$P_{outage} = P(P_{TX} > P_{max}), \tag{3-25}$$

where P_{max} is the maximum output power of handset.

The greater the distance of a mobile handset from its home BS, the greater the probability of the user experiencing service outage. Therefore, as in [26], the coverage of a cell can be expressed as

$$d_{\mathrm{cov}} = \max\{ r : P_{outage} \leq \delta \}, \tag{3-26}$$

where δ is an acceptable level for outage probability. In this study, δ is set to 0.1. In the next chapter, we will present the results for the reduction in cell coverage caused by CCI.

CHAPTER FOUR: NUMERICAL RESULT

The numerical result shown in this chapter comes from simulations. In the downlink CCI analysis, the performance of different FFR schemes are analyzed. To reduce CCI in the downlink and to improve the network capacity, FFR schemes allocate different power levels to cell-interior users and cell-edge users. In the uplink CCI analysis, the handset output power limitation is taken into consideration. The cell coverage affected by CCI can be ascertained through service outage probability analysis. A radio network with a total of 19 BSs is employed in the study. The cell layout of our wireless network is presented in Figure 4.1.

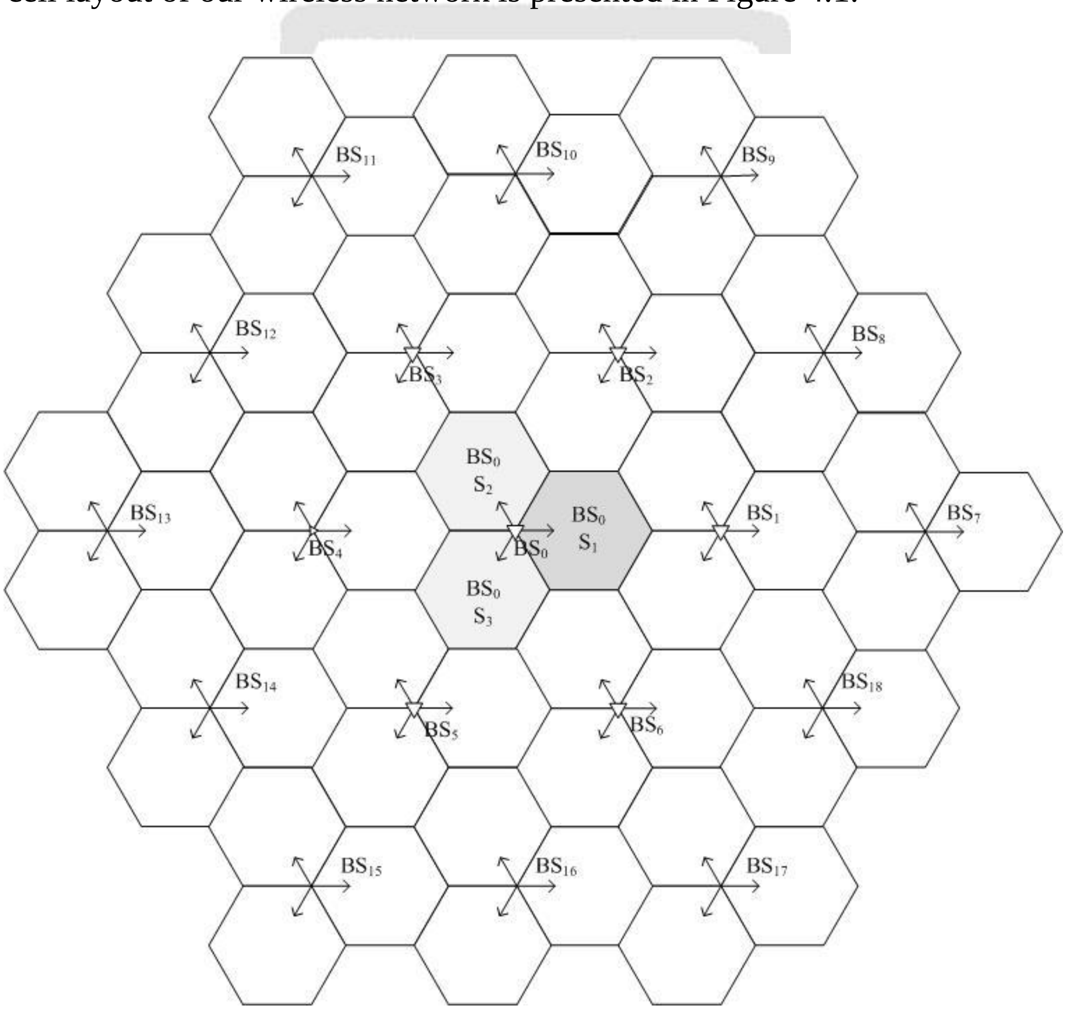

Figure 4.1 Cell layout of the wireless network.

4G networks can operate in multiple frequency band, in which the carrier frequency changes the propagation model. Hata's propagation formulation, suited to the frequency band from 150 to 1500 MHz, for an urban area is [40]

$$PL_{urban(dB)}=69.55+26.16\log_{10}(f)-13.82\log_{10}(H_{BS})$$

$$+(44.9-6.55\log_{10}(H_{BS}))\log_{10}(r)-a(H_{MS}), \tag{4-1}$$

where H_{BS} is the antenna height of BS and H_{MS} is the antenna height of MS. The parameter r is expressed in kilometers, and f is expressed in megahertz. In a big city, the $a(H_{MS})$ would be

$$a(H_{MS})=3.2(\log_{10}(11.75H_{MS}))^2-4.97.$$

Hata's formulation [40] for a rural area is

$$PL_{rural\ (dB)}= PL_{urban\ (dB)}-4.78(\log_{10}(f))^2+18.33\log_{10}(f)-40.94. \tag{4-2}$$

The extended COST-231-Hata model is based on the frequency band from 1500 to 2000 MHz. In an urban environment with carrier frequency 2000 MHz, the propagation model is [40]

$$PL_{urban(dB)}=128.1+37.6\log_{10}(r)+21\log_{10}(f_c/2), \tag{4-3}$$

where r is expressed in kilometers and f_c is expressed in gigahertz. In a rural area, the extended COST231-Hata propagation model is

$$PL_{rural(dB)}=46.3+33.9\log_{10}(f)-13.82\log_{10}(H_{BS})$$

$$+(44.9-6.55\log_{10}(H_{BS}))\log_{10}(r)-a(H_{MS}), \tag{4-4}$$

and the $a(H_{MS})$ equals the $a(H_{MS})$ in Hata's formulation.

When the carrier frequency is up to 2.5 GHz, the COST-231-Hata model for urban area with a frequency scaling factor is used as a propagation model [39]. The propagation formulation is

$$PL_{urban(dB)}=(44.9-6.55\log_{10}(H_{BS}))\log_{10}(\,r\,)$$

$$+26.46+5.83\log_{10}(H_{BS})+26\log_{10}(\,f_c/2), \qquad (4\text{-}5)$$

where r is expressed in meters and f_c is expressed in gigahertz. The propagation model use in rural area on frequency 2.5 GHz is [39]:

$$PL_{rural(dB)}=PL_{urban(dB)}-2(1.5528+\log_{10}(\,f_c\,))^2-5.4, \qquad (4\text{-}6)$$

When H_{BS} is 30 m and the H_{MS} is 1.5 m, the propagation models can be simplified as shown as Table 4.1.

Table 4.1 The propagation model in different frequency bands

900 MHz	
$PL_{urban(dB)}=49.15+35.2\log_{10}(\,r\,)+26.16\log_{10}(\,f\,)$	r=kilometers, f=MHz
$PL_{rural(dB)}=8.2+35.2\log_{10}(\,r\,)+44.49\log_{10}(\,f\,)-4.78(\log_{10}(\,f\,))^2$	
2000 MHz	
$PL_{urban(dB)}=128.1+37.6\log_{10}(\,r\,)+21\log_{10}(\,f_c/2\,)$	r=kilometers, f_c=GHz
$PL_{rural(dB)}=25.9+35.2\log_{10}(\,r\,)+33.9\log_{10}(\,f\,)$	r=kilometers, f=MHz
2500 MHz	
$PL_{urban(dB)}=35.07+35.2\log_{10}(\,r\,)+26\log_{10}(\,f_c/2\,)$	r=meters, f_c=GHz
$PL_{rural(dB)}=PL_{urban(dB)}-2(1.5528+\log_{10}(\,f_c\,))^2-5.4$	

Source: [39], [40]

4.1 The FFR Schemes Analysis in Downlink CCI

Due to the limited spectrum, we need to develop frequency reuse schemes and assign frequency bands to each cell or sector. Applying the propagation model to each transmission link, we can evaluate the SINR for mobile users, and then calculate the throughput performance.

We focus on the cell performance of sector S_1 because of the symmetry of cell layout. The other sectors (cells) may contribute considerable powers of CCI. For downlink communications, mobile stations are the victims and the interfering signals come from BSs. The CCI powers received at MSs in sector S_1 can be calculated based on a propagation model including path loss and shadow fading effect. The MSs in S_1 can receive only a little power radiated from the BS antennas at S_2 or S_3 due to their directional antenna pattern.

Two typical FFR deployment schemes have been presented in the literature [42], [43]: partial frequency reuse (PFR) and soft frequency reuse (SFR). In the PFR scheme, a reuse factor of three is used in cell-edge regions and a reuse factor of one in cell-center regions. PFR can improve cell-edge performance but with severe penalty to the overall throughput. In the SFR scheme, the cell-edge region uses 1/3 of the available bandwidth and forms a structure of cluster size of 3. The cell-interior region is assigned the frequencies used in the cell-edge regions of adjacent cells. High transmission power is allocated to the cell-edge users.

In this section, two new schemes are proposed to improve the system performance of existing FFR schemes. One proposed scheme is based on typical PFR, and the other is based on SFR. This section analyzes the CCI power received by mobile stations that are the victims of downlink transmissions. The CCI signals received by cell-interior and cell-edge users are calculated and compared using different FFR schemes. Average throughput is adopted to evaluate the performance of FFR schemes. Random user locations and the shadow fading propagation model are employed to calculate the average SINRs of mobile users. Different FFR schemes are also used to discuss the throughput performance of cell-interior and cell-edge users. In addition, the impact of various propagation environments (urban and rural) on FFR performance is investigated. The research results provide an overall picture of system capacity when FFR is employed in wireless communication networks.

To reduce CCI in the downlink, FFR schemes allocate different power levels to cell-interior users and cell-edge users.

The transmission power of BS can be expressed as

$$P_t = \begin{cases} P_c, & \text{for interior area} \\ P_e, & \text{for edge area} \end{cases}. \tag{4-7}$$

In general, $P_c < P_e$. Assume that a mobile station MS_0 is within the coverage of BS_0.

There are two main FFR schemes, PFR and SFR. In the PFR scheme, the whole channel bandwidth is divided into four groups of subbands. One of the four groups is assigned for the center region in each cell. The other three groups are used for the edge regions.

A typical PFR layout is shown in Figure 4.2 (a). The three sectors of a BS use three different subband groups. This frequency assignment pattern is reused for every

BS.

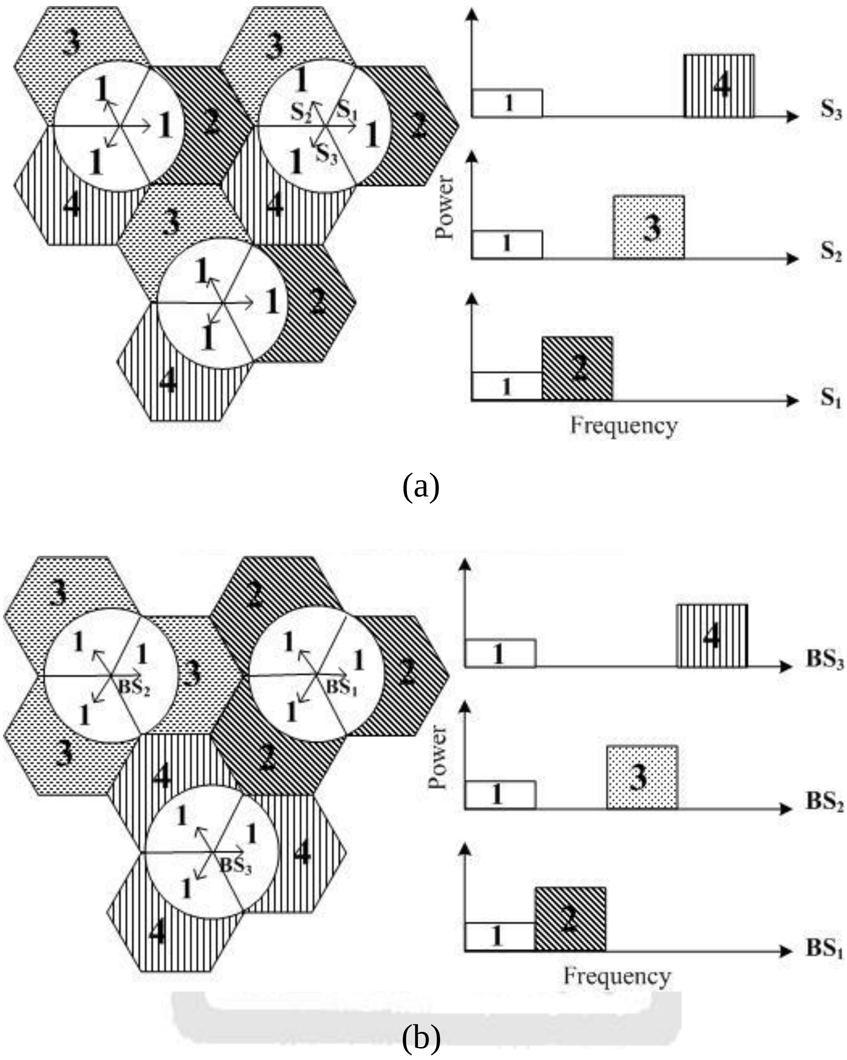

Figure 4.2 Partial frequency reuse schemes; (a) typical, (b) proposed.

To enhance the throughput performance, we propose a new partial frequency reuse scheme in which the three sectors of a BS use the same subband group. This frequency assignment pattern is repeated for every three BSs. The proposed partial frequency reuse is presented in Figure 4.2 (b). Since cell-interior users in general suffer from less path loss, BSs could transmit small power levels for the interior users.

Figure 4.3 shows how the CCI mitigation effects of proposed PFR for edge users. In Figure 4.3, the BS antennas in the sectors with slanted lines will radiate interference signals to the edge MSs in the reference sector S_1. The proposed partial frequency reuse scheme can increase the distance between two co-channel communication links and hence reduce the CCI. Figure 4.3 (a) and 4.3 (b) shows how the number of interference sources can be reduced from eight to six by this proposed partial frequency reuse.

In the SFR scheme, the system channel bandwidth is divided into three groups. Figure 4.4 (a) presents the typical soft frequency reuse scheme. Each sector contains all three subband groups, in which two are assigned for the region close to BS and the other one is assigned for cell-edge region. From a BS point of view, the three sectors use all three subband groups.

In the proposed soft frequency reuse scheme, as shown in Figure 4.4 (b), the three edge regions of a BS shares the same subband group. This frequency assignment pattern is repeated for every three BSs.

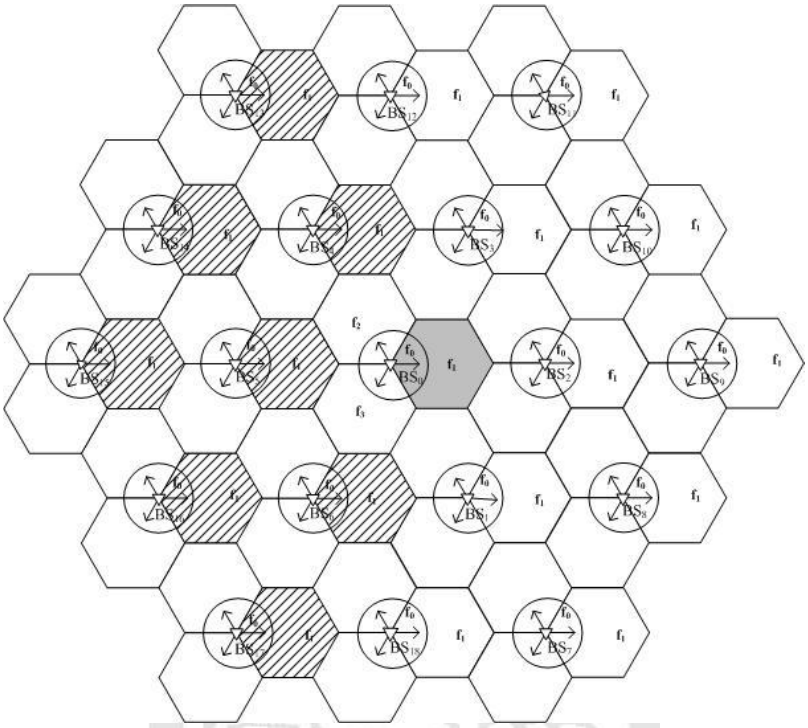

(a)

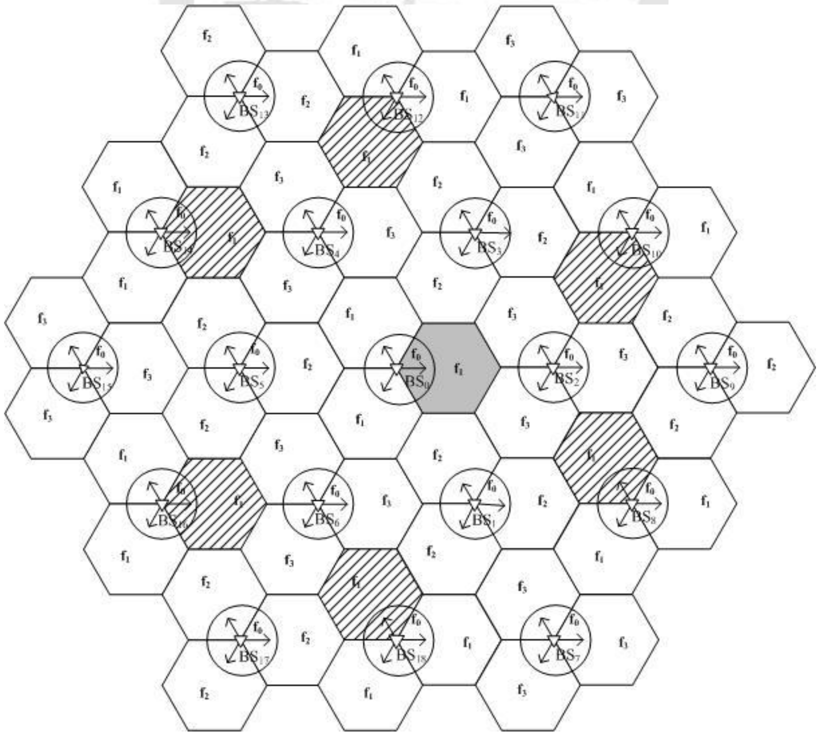

(b)

Figure 4.3 Interference sources to edge users; (a) typical PFR, (b) proposed PFR.

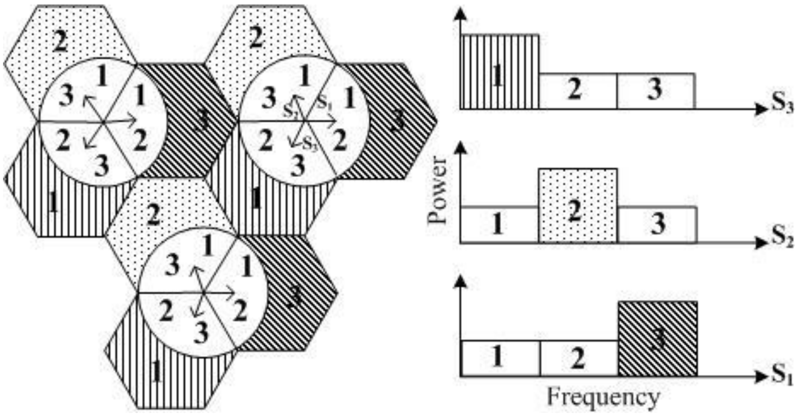

(a)

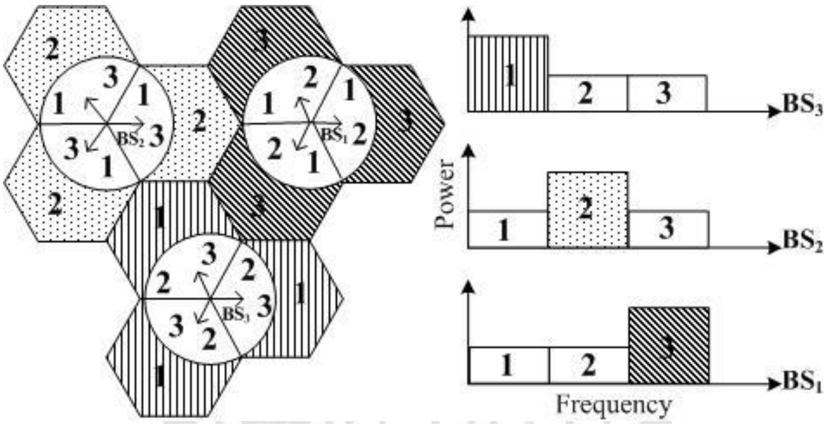

(b)

Figure 4.4 Soft frequency reuse schemes; (a) typical, (b) proposed.

Figure 4.5 shows the effect of the proposed SFR on interference source mitigation to edge users. Vertical or crisscross lines indicate that the BS antenna in this sector is a low-power (P_c) or a high-power (P_e) interference source for the edge MSs in reference sector S_1. In our analysis of 19 BSs, Figure 4.5 (a) shows the typical SFR contains three high-power interference sources and three low-power interference sources in the first-tier and five high-power interference sources and seven low-power interference sources in the second-tier. It can be found in Figure 4.5 (b) that the proposed SFR reduces the interference to six low-power sources in the first-tier.

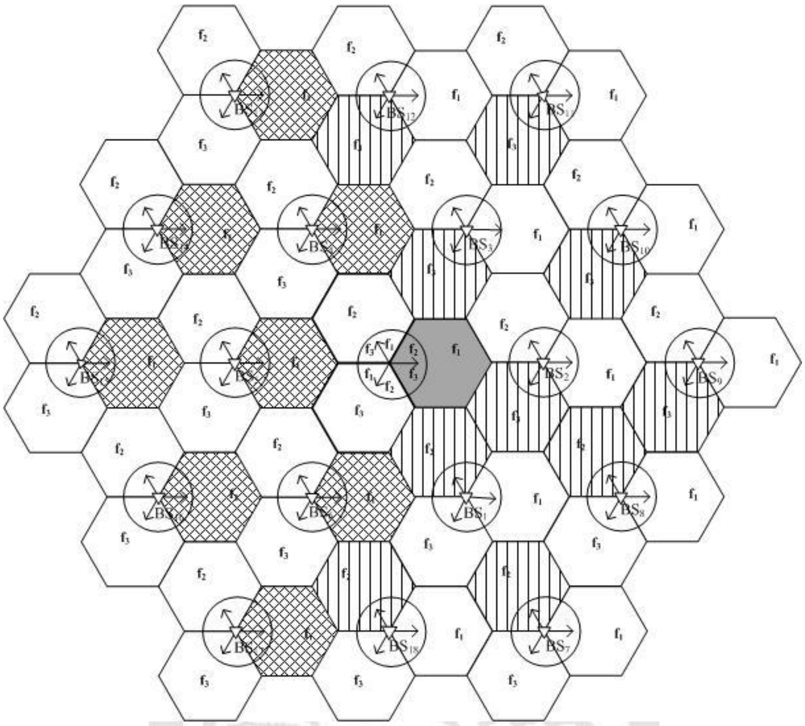

(a)

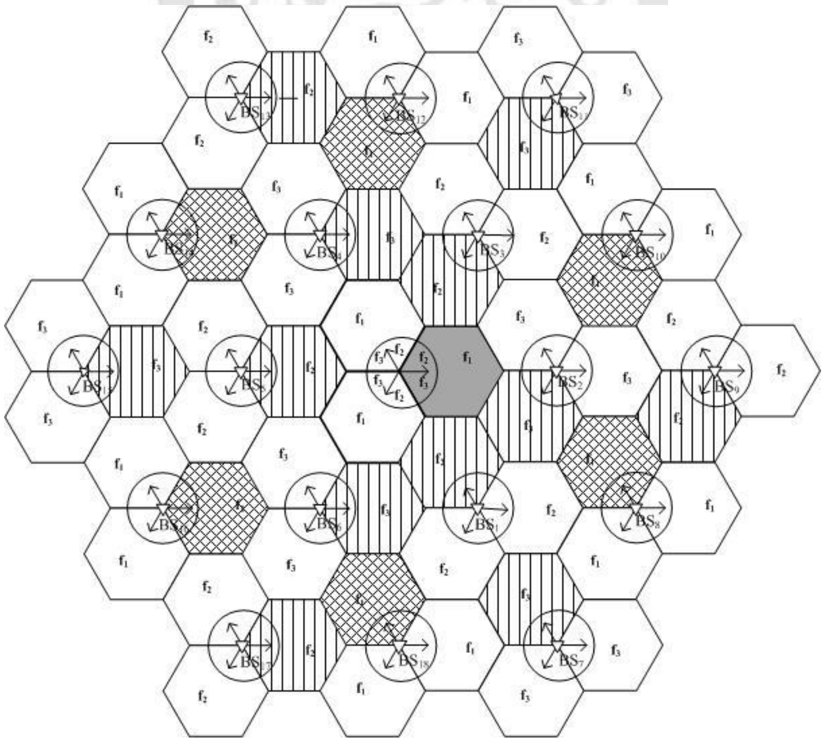

(b)

Figure 4.5 Interference sources to edge users; (a) typical SFR, (b) proposed SFR.

The primary parameters used in the numerical calculations are listed in Table 4.2. Although the 4G networks can provide flexible channel bandwidth, we use a channel bandwidth of 10 MHz, which consists of 600 subcarriers for data transmissions. The channel bandwidth can provide 50 RBs. Each RB consists of 12 subcarriers, and each subcarrier has a bandwidth of 15 kHz. We also assume that the available spectrum for downlink is in the LTE band 1 (2110-2170 MHz). The inter-site distance is set to 750 m in the urban area and 1500 m in the rural area. Each site has three sectors, and each sector is equipped with a directional antenna with the pattern shown in Figure 3.3.

Table 4.2 Parameter values in numerical calculations for downlink

Parameters	**Values**
Frequency band	2140 MHz
Channel bandwidth	10 MHz
Total resource blocks	50
Subcarrier per resource block	12
BS maximum transmission power	46 dBm
BS transmission power to interior area	33 dBm
Subcarriers bandwidth	15 kHz
BS antenna gain	15 dBi
MS antenna gain	0 dBi
MS noise figure	9 dB
Standard deviation of fading	8 dB
BS antenna height	30 m
MS antenna height	1.5 m
Site to site distance	750m/1500m (urban/rural)

In this section, the path loss formulas are applied to urban and rural areas (on frequency band 1, 2000MHz) for macro cell configuration, as shown in Table 4.1. The gap between the path loss values in urban and rural areas is shown in Figure 4.6. The path loss in the urban environment is about 20 dB greater than that in rural area. The carrier frequency is set to 2.14 GHz (or 2140 MHz).

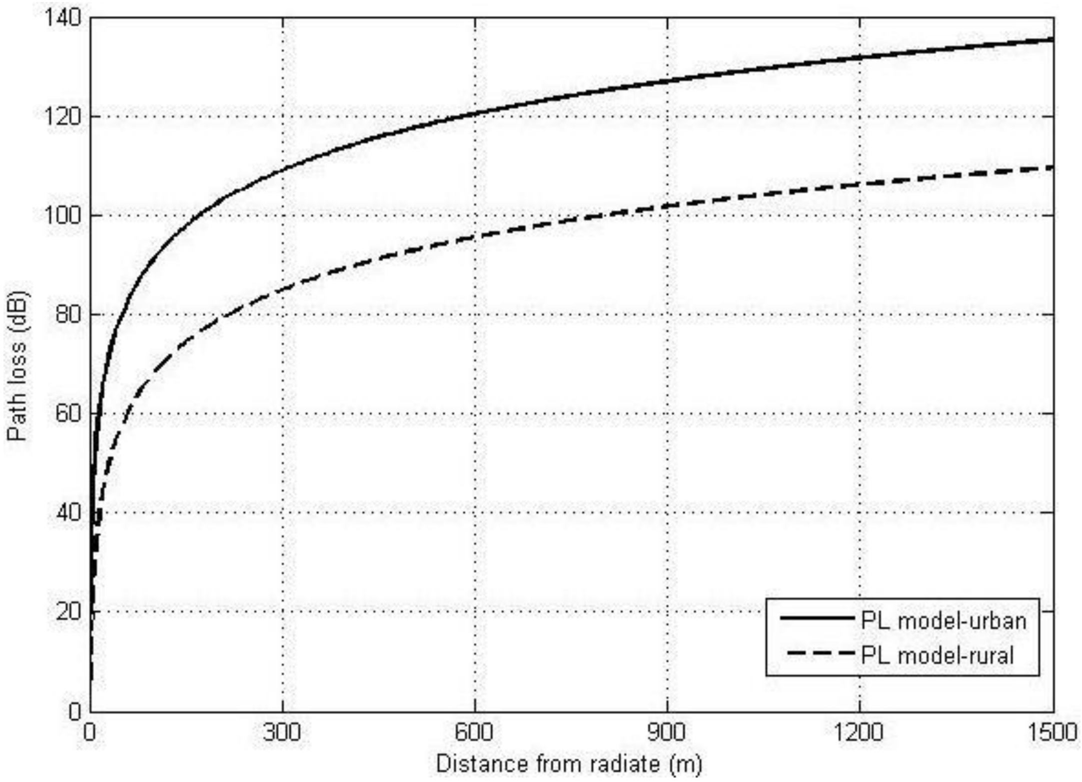

Figure 4.6 Two path loss models.

We evaluate the throughput performance of FFR schemes in this study. Extensive simulations are performed using the Monte Carlo snapshot method. Mobile users are randomly located in the coverage of each cell. Each mobile user is randomly located in 1000 different positions. For each position, we obtain a total CCI value from all interference sources to that mobile user, and then calculate the

SINR and throughput for that mobile user. After calculating the mobile user with 1000 different locations' throughput, we can get the average throughput for a frequency channel.

The threshold radius to separate the center region and edge region is set as 0.6 of the cell radius [38]. It is 225 m in urban environment and 450 m in rural environment. The maximum power of a BS is 46 dBm [5], and the radiation power to interior area is set as 33 dBm to simplify the simulation. Note that the larger interior radiated power can increase the received power to center-users, but the interference power from adjacent cells will rise too. Assume that the transmission power is uniformly allocated to each RB. Because there are 50 RBs in the wireless network, an RB can obtain maximum radiation power of 29 dBm. As mentioned in (4-7), we need to allocate less power to the links for cell-interior users to reduce CCI. Hence, P_c is set to 16 dBm and P_e is 29 dBm.

The reference BS is assumed to operate in a full load condition in which all available RBs are used. Each downlink with a RB in the reference site may receive CCI from adjacent BSs if the same RB is also used in any other sites. To analyze the influence of traffic load on CCI, we set different levels of traffic load for the adjacent BSs. Note that the traffic load is defined as the number of used RBs divided by the number of available RBs.

First, we need to examine the CCI power received by cell-interior users and edge users. Figure 4.7 presents the average CCI power received at MSs as the function of traffic load for different FFR schemes. As expected, the CCI power is increased when the traffic load increases.

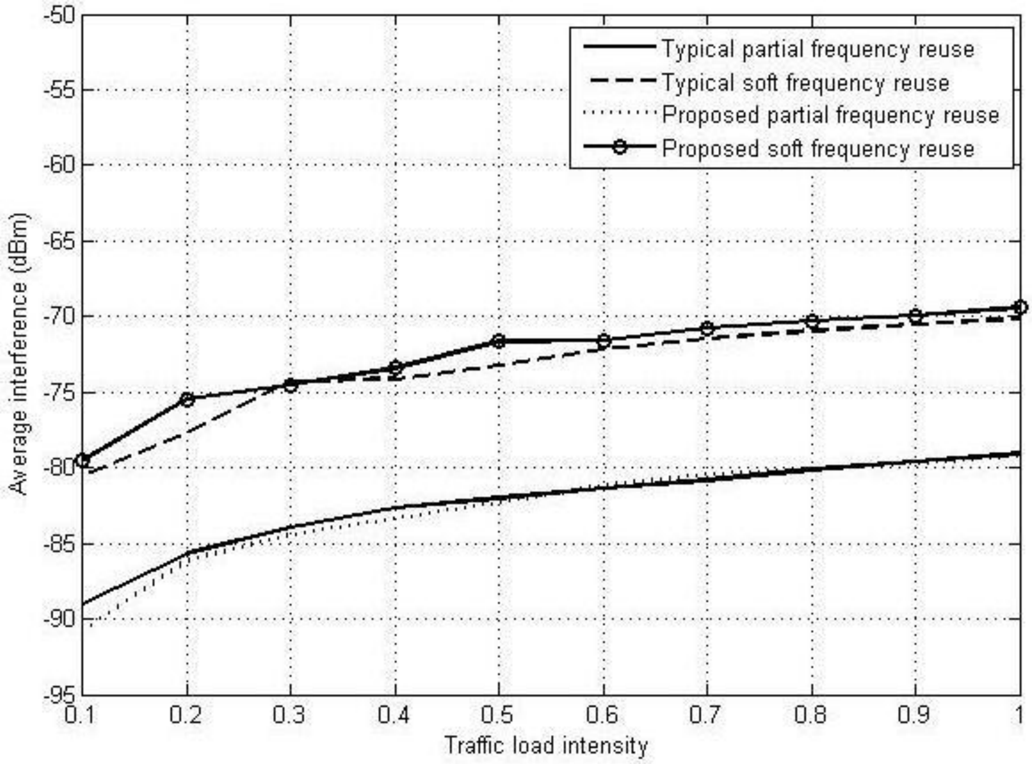

(a)

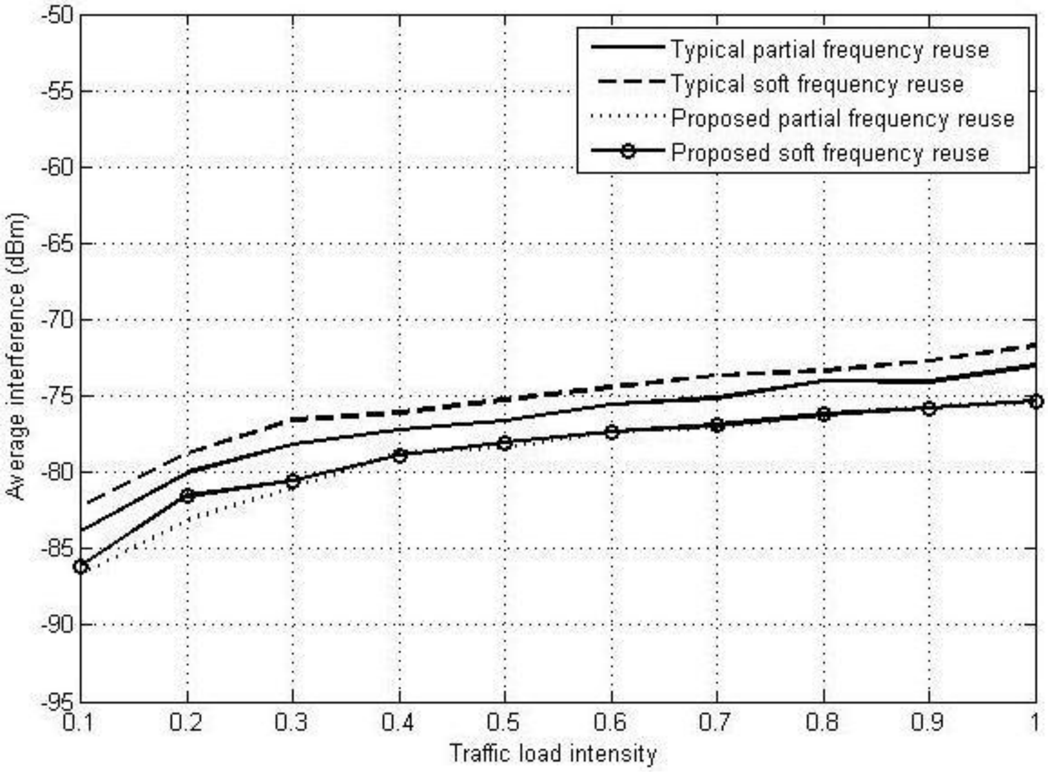

(b)

Figure 4.7 Co-channel interference power in urban environment; (a) center users, (b) edge users.

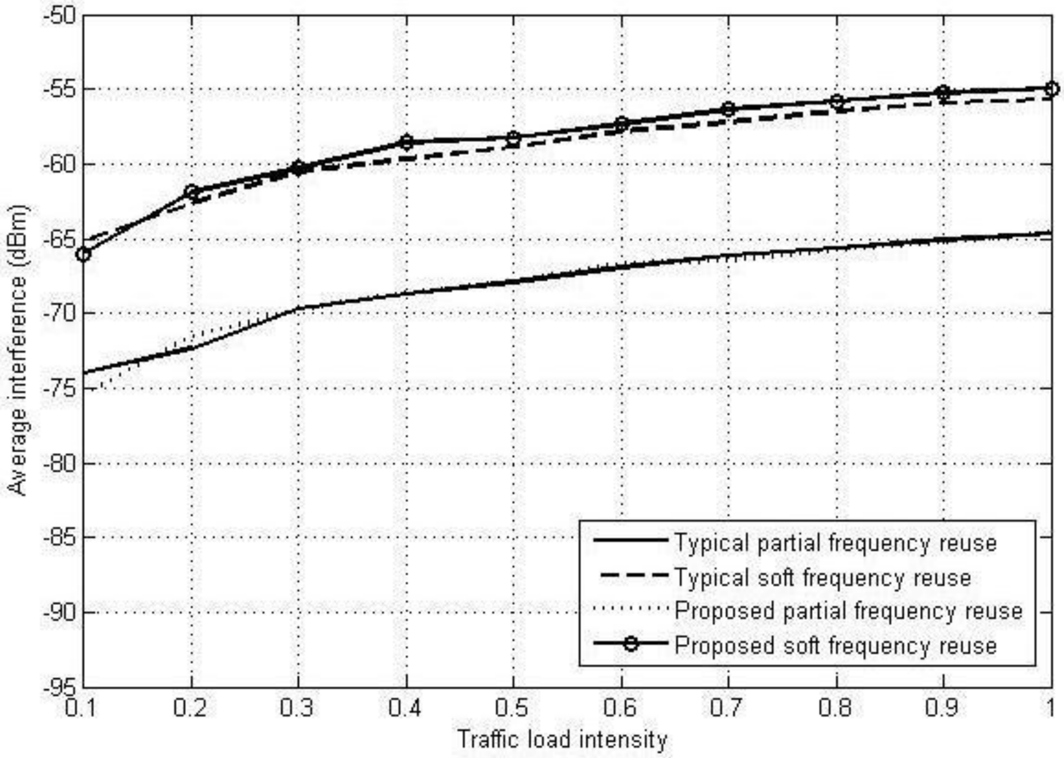

(a)

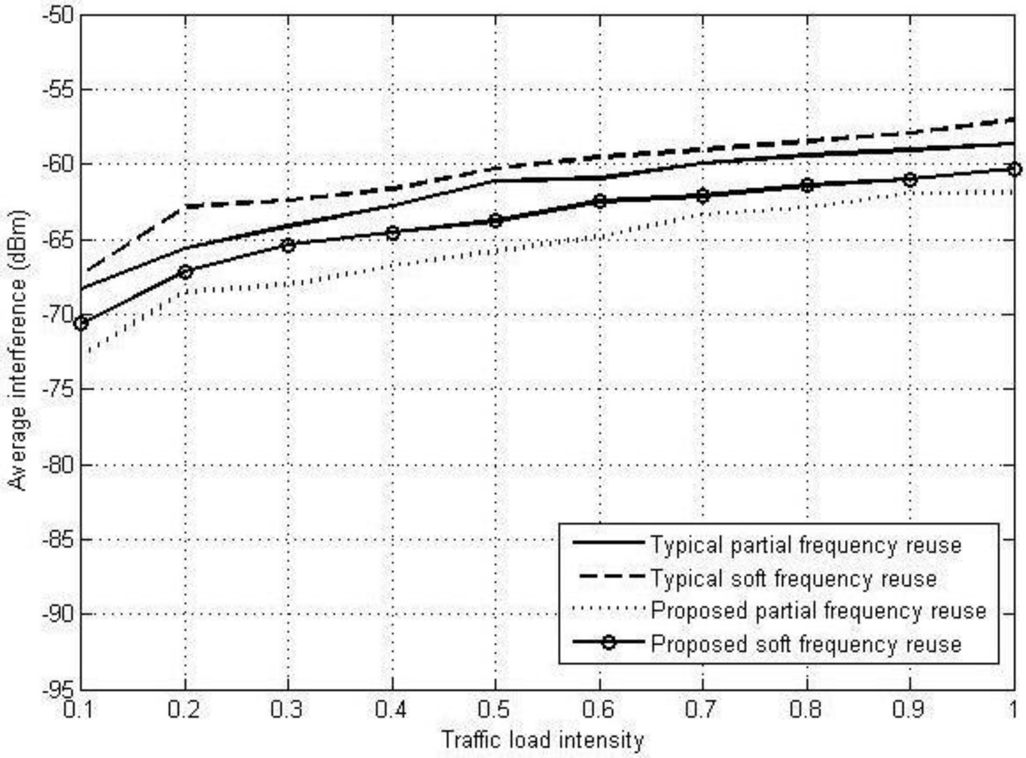

(b)

Figure 4.8 Co-channel interference power in rural environment; (a) center users, (b) edge users.

We can observe that the proposed soft-FFR can reduce edge user CCI by 50%, about 3 dB, compared to the typical soft-FFR. Our partial-FFR has a similar result. Moreover, in the cell-interior region, the two partial-FFR schemes cause less CCI than the soft-FFR schemes. Figure 4.8 shows the CCI power in a rural environment. Due to the smaller path loss in the rural environment, the victims receive more CCI power, particularly the cell-edge users. The proposed FFR schemes still can reduce CCI power to edge user by 50% in rural environment.

In the presence of CCI, we can calculate the SINR for each link. Figure 4.9 presents the cumulative density function (CDF) of SINR using the proposed soft-FFR. It can be observed that high traffic loads lead to more reduction in SINR. For instance, if 30% of RBs are used, the average SINR for edge users is about 18 dB. When the traffic load increases to 80%, the average SINR decreases dramatically to about 10 dB. Figure 4.9 also shows that the cell-edge users see a greater SINR than do cell-interior users when the proposed SFR is used.

After obtaining SINR for each link, we can calculate the normalized throughput from (3-10). The user-normalized throughputs for the case of an urban environment are presented in Figure 4.10. Both the proposed partial-FFR and proposed soft-FFR can significantly enhance edge-user throughput, as shown in Figure 4.10 (b). We can also observe from Figure 4.10 (a) that the partial-FFR scheme provides better throughput performance for cell-interior users than soft-FFR does. Similar results can be found in Figure 4.11 for the rural environment.

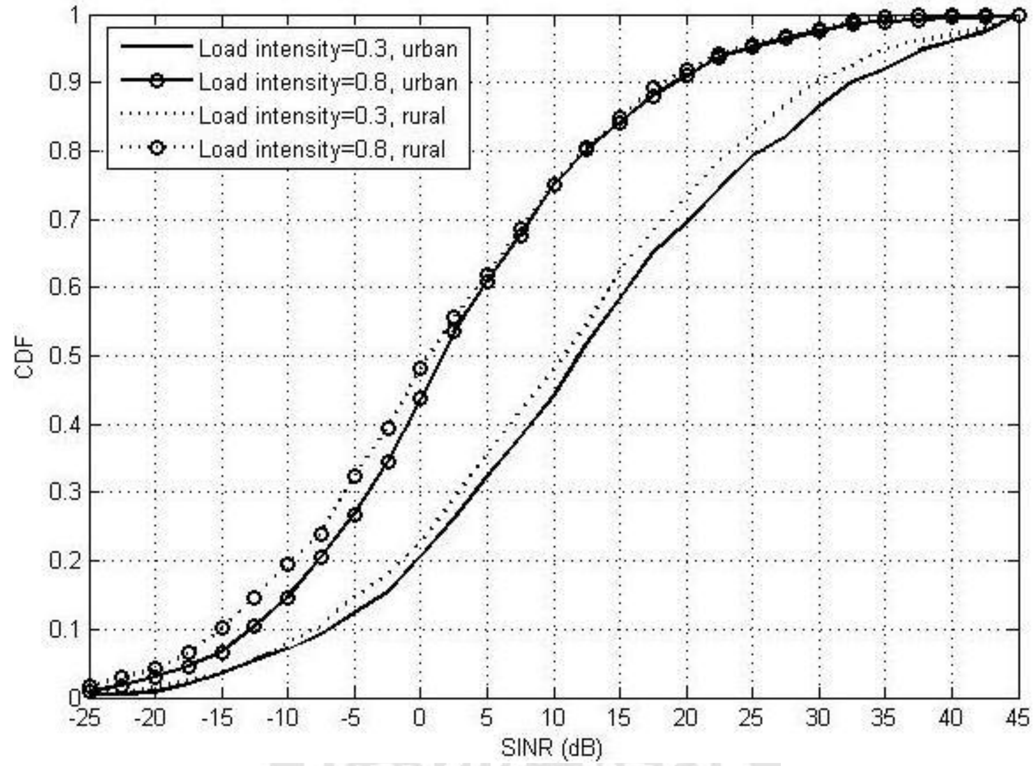

(a)

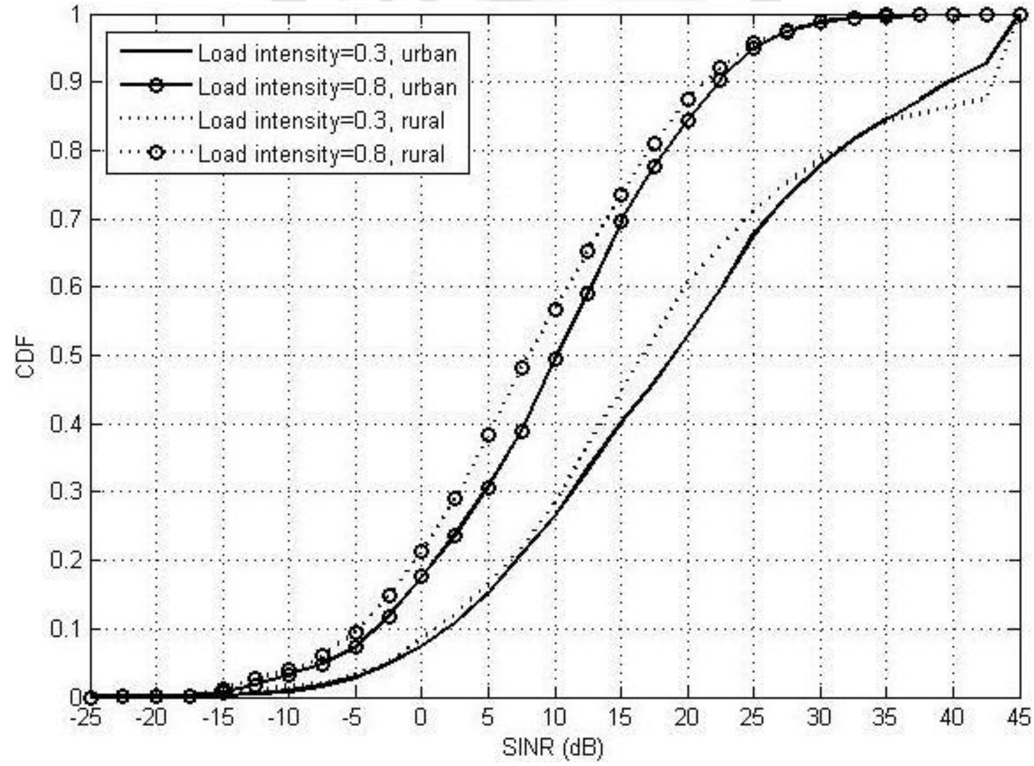

(b)

Figure 4.9 Cumulative density function of SINR with proposed soft-FFR; (a) center users, (b) edge users.

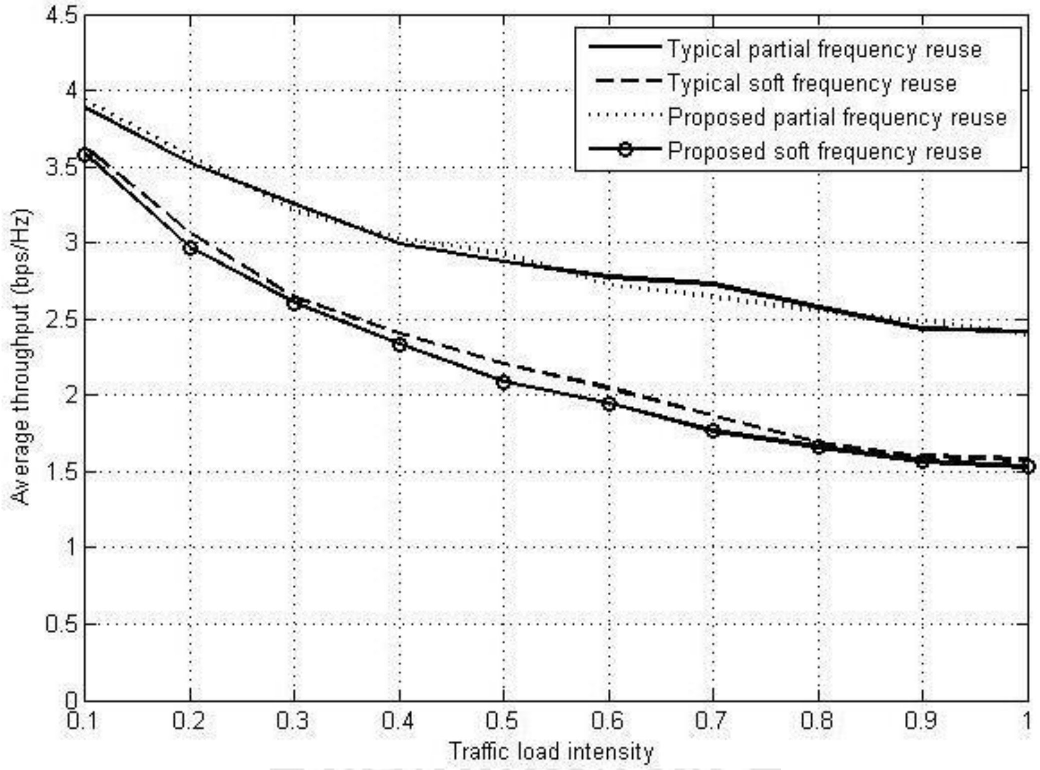

(a)

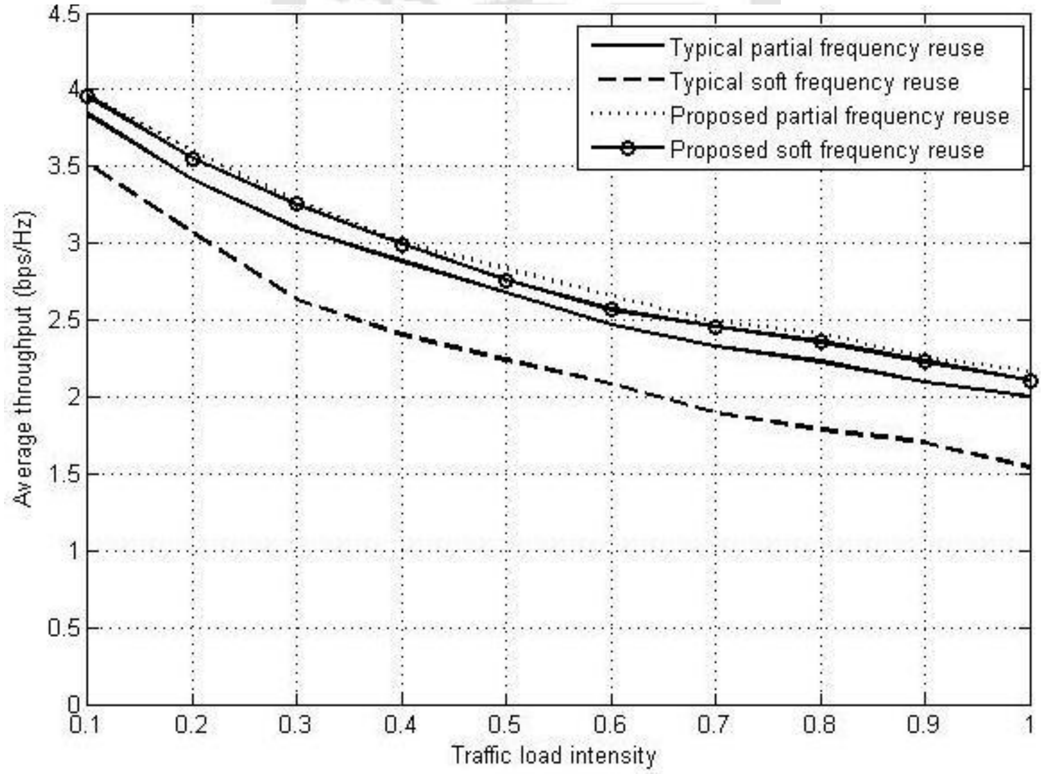

(b)

Figure 4.10 Average throughput in urban environment; (a) center users, (b) edge users.

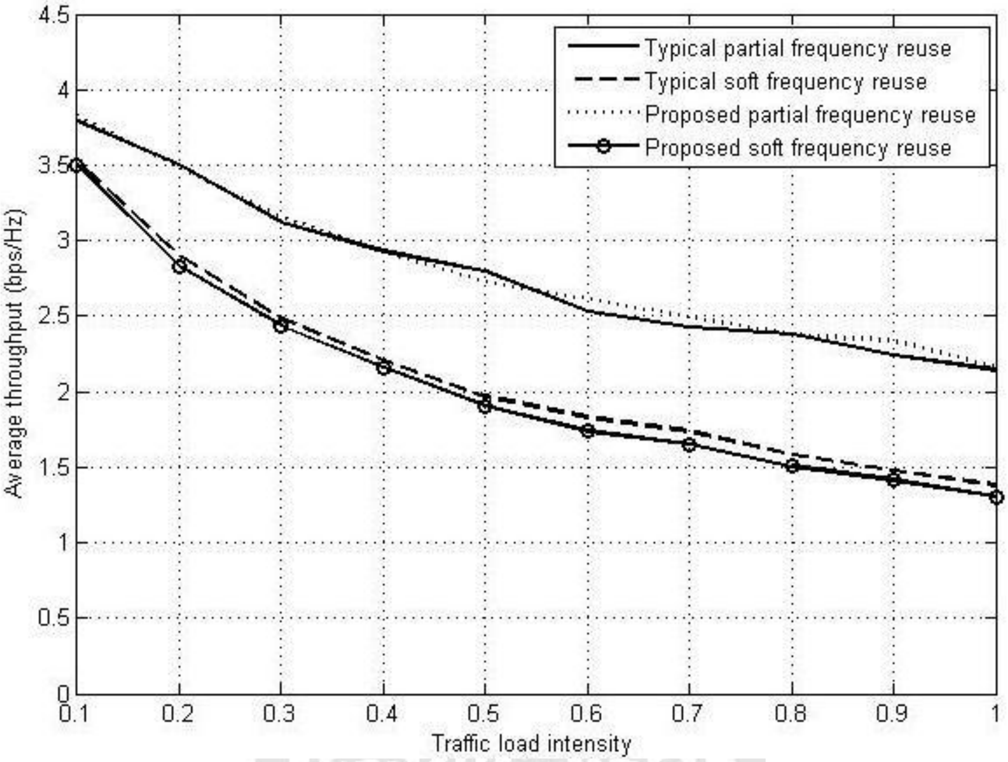

(a)

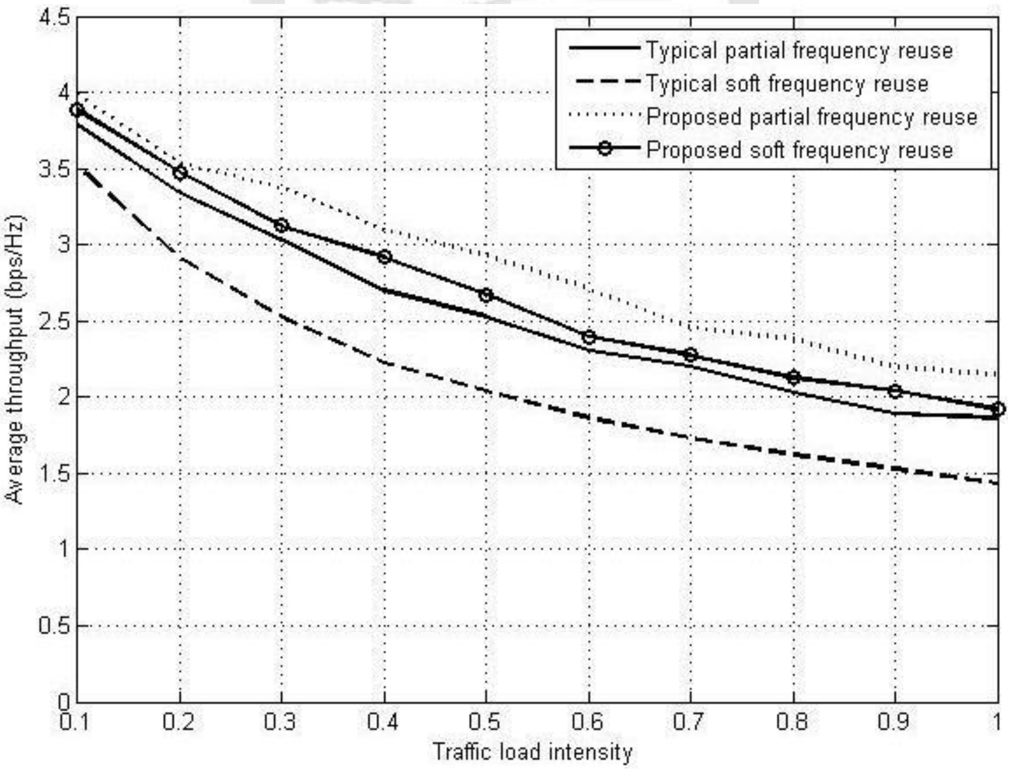

(b)

Figure 4.11 Average throughput in rural environment; (a) center users, (b) edge users.

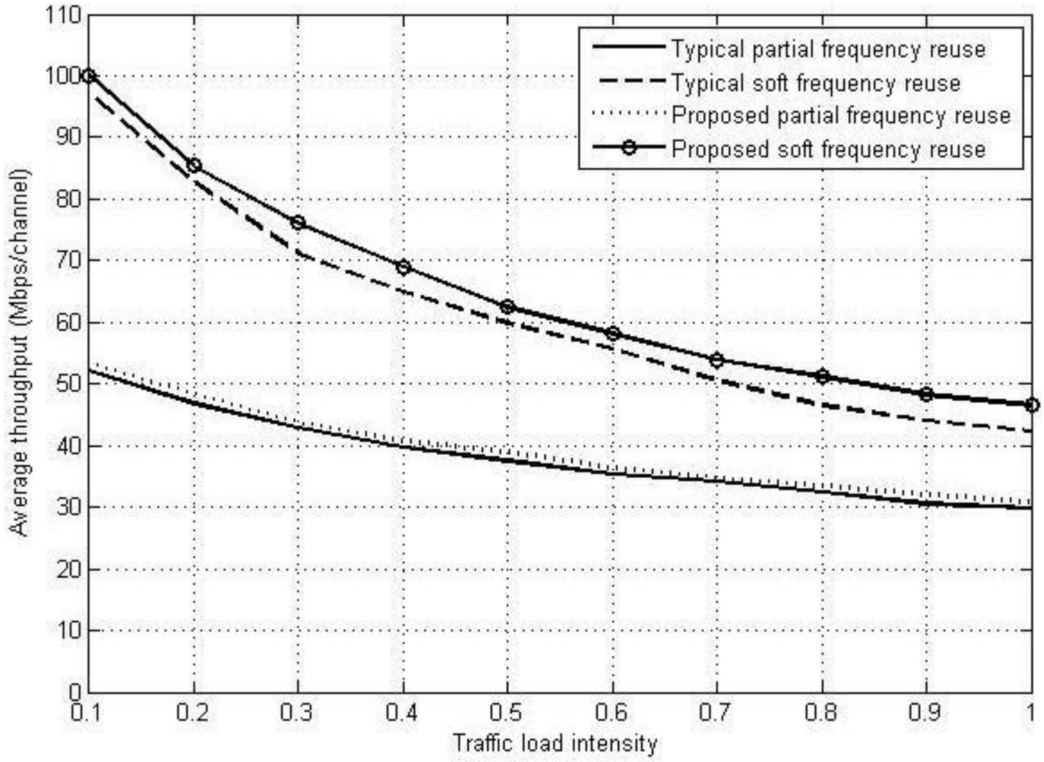

(a)

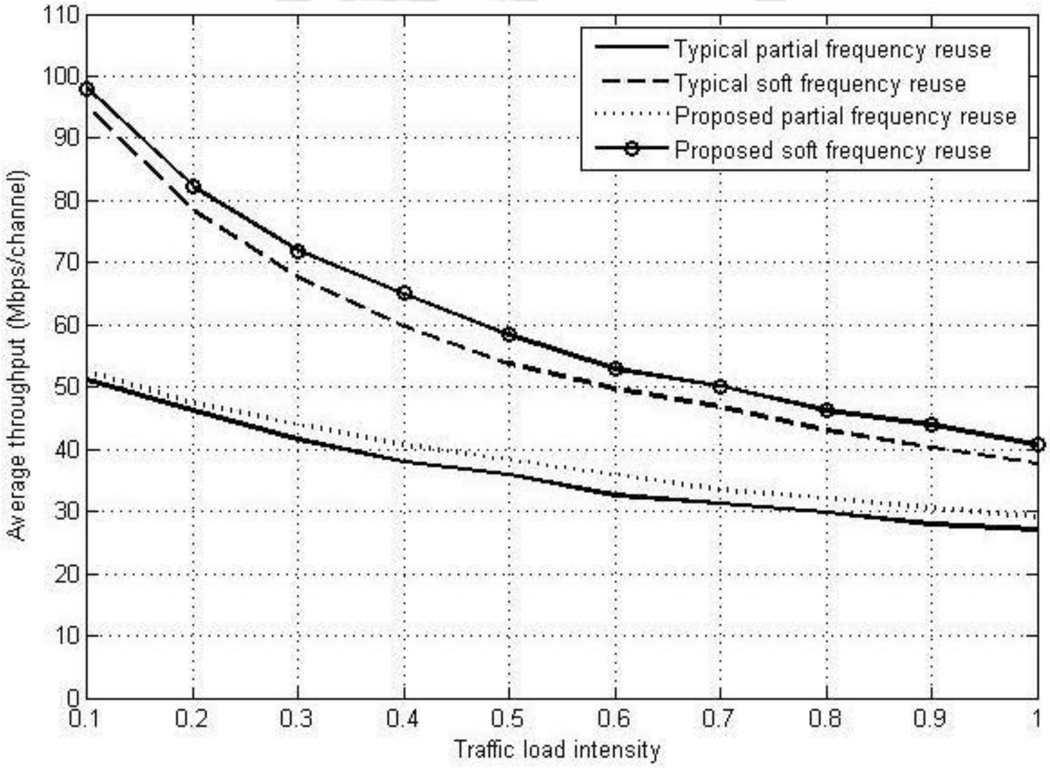

(b)

Figure 4.12 Average channel capacity of the reference site; (a) urban environment, (b) rural environment.

Figure 4.12 shows the average channel capacity for the reference BS, which consists of three sectors. The channel bandwidth used in the cellular network is 10 MHz. Among the four FFR schemes, the proposed soft-FFR can provide the highest channel throughput. Compared to the typical partial-FFR, the proposed partial-FFR has no significant improvement of channel throughput, but it can improve the throughput performance for cell-edge users. From Figure 4.12 we also find that if the system is operated in interference-free condition (traffic load=0), the average channel throughput can reach up to 100 Mbps/channel. When the interfering BSs are in fully loaded operation (traffic load=1), the total throughput reduces to about 30 Mbps/channel with proposed PFR and 45 Mbps/channel with proposed SFR due to the inter-cell CCI. This result reveals that the CCI can significantly reduce the system throughput when the cells are operated in a fully loaded situation.

Table 4.3 to Table 4.5 summarizes the performances about interference reduce and throughput increase to edge users by proposed PFR and proposed SFR schemes. Table 4.3 summarizes the interference power mitigation performance of proposed PFR to edge users. Compared to the typical PFR, the proposed PFR can reduce interference power by 39% in an urban environment and 57% in a rural environment. No matter which environment, the proposed SFR can reduce interference power to edge users by over 50% compared to typical SFR, as summarized in Table 4.4. Regarding system capacity, Table 4.5 lists the proposed FFR schemes' performance of edge users. The proposed PFR and proposed SFR can increase the edge user average throughput by 6% to 27%.

Table 4.3 Average interference power mitigation by proposed partial FFR schemes

	$\frac{\text{Proposed PFR}}{\text{Typical PFR}}$ (mW)	Typical PFR-Proposed PFR (dB)
Urban	39%	2.2
Rural	57%	3.7

Table 4.4 Average interference power mitigation by proposed soft FFR schemes

	$\frac{\text{Proposed PFR}}{\text{Typical PFR}}$ (mW)	Typical SFR-Proposed SFR (dB)
Urban	52%	3.2
Rural	52%	3.2

Table 4.5 Average throughput increase by proposed FFR schemes

	Proposed SFR (compared to typical SFR)	Proposed PFR (compared to typical PFR)
Urban	25%	6%
Rural	27%	13%

4.2 The Cell Coverage Analysis in Uplink CCI

In our simulations, the values of primary parameters are set mainly according to the evaluation methodology document for IEEE 802.16m [44]. Table 4.6 lists the parameter values used in our numerical calculations. The channel bandwidth assigned to each sector is 10 MHz. The fast Fourier transform (FFT) size is set to 1024, corresponding to 1024 subcarriers. The subcarrier spacing is about 11 kHz. In the 802.16m standard, a large part of the available subcarriers are partitioned into 48 subchannels. Each subchannel accommodates 18 subcarriers and has an effective bandwidth of 176 kHz. According to the 802.16m standard, a mobile node can obtain several subchannels for its data transmission needs.

In the uplink analysis, we assume that the BS's directional antennas are well designed and the antennas receive the signals in the 120° area only. From the cell layout of our analysis network shown in Figure 4.1, the scope of uplink analysis will narrow to 9 BSs. Figure 4.13 shows the uplink analysis cell layout. The mobile users in striped cells will radiate interference signals to victim BS_0.

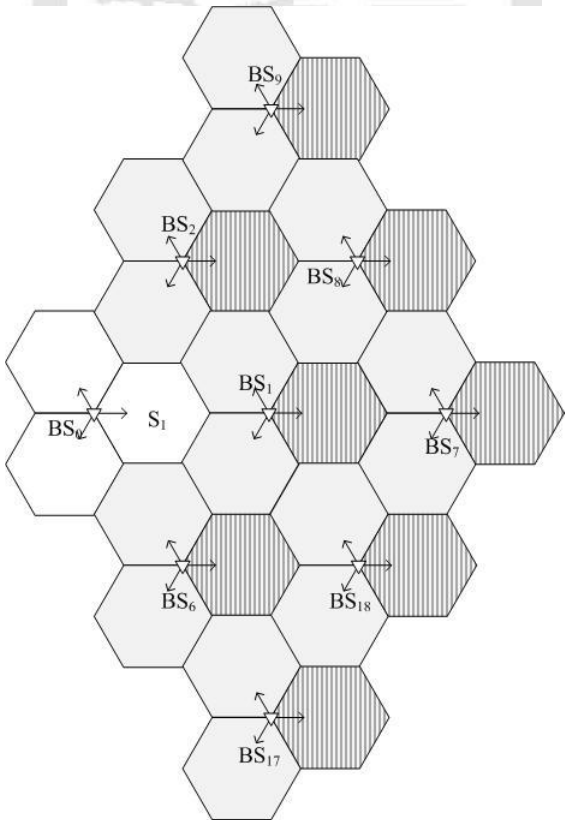

Figure 4.13 Cell layout in uplink interference analysis

Table 4.6 Parameter values in numerical calculations for uplink

Parameters	**Values**
Frequency band	2.5 GHz
Sector bandwidth	10 MHz/sector
FFT size	1024
Frequency reuse factor	3
Subchannel bandwidth	198 kHz
BS antenna gain	15.0 dBi
MS antenna gain	0 dBi
BS noise figure	5 dB
Standard deviation of fading	8 dB
BS antenna height	30 m
MS antenna height	1.5 m
Handset output power	23 dBm
Site to site distance	750 m

The values of required SINR for different modulation schemes are listed in Table 4.7 [2]. In this study, we use the COST-231 Hata propagation model to fit the 2.5 GHz in urban area. This model corresponds to $C = 10^{-3.77}$ and $\mu = 3.5$ in equations (3-14) or (3-15) if the carrier frequency f_c is 2.5 GHz.

Table 4.7 Receiver SINR assumptions

Modulation	**Coding rate**	**Required SINR (dB)**
QPSK	1/2	6
QPSK	3/4	8.5
16-QAM	1/2	11.5
16-QAM	3/4	15

First, we examine the impact of CCI on the service outage probability. Consider a single subchannel assigned in each sector. Figure 4.13 presents the outage probability as a function of the distance between BS_0 and MS_0. We assume θ_0=60°, and every MS is assigned one subchannel in the simulations. The communication link has a significant increment in outage probability due to the co-channel signals from other cells' mobile users. This outage probability increment will lead to cell coverage reduction. In other words, the CCI will make it difficult for mobile users at cell boundaries to maintain necessary link quality. Assume the acceptable level for outage probability is set to 0.1 for the calculation of cell coverage. We can observe from Figure 4.13 that the cell coverage is reduced to about 160 m for SINR=11.5 dB due to the CCI when the handset maximum output power set as 1W.

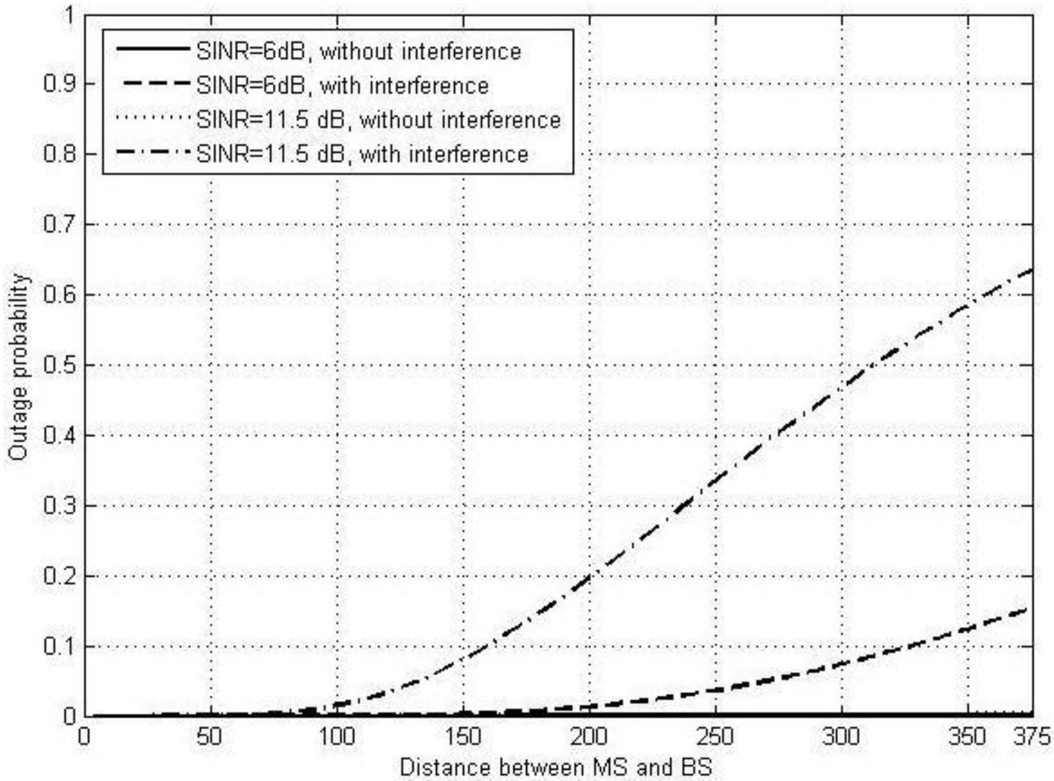

Figure 4.13 CCI impact on outage probability with maximum output power of 1 W.

If mobile users need to send a large amount of data, they must use more subchannels for their transmissions. In this heavy traffic situation, the CCI may have a more serious impact on the service outage probability. Figure 4.14 shows the influence of subchannel quantity assigned to mobile users on outage probability in the presence of CCI. We assume the mobile users who use co-channel f_1 get the same number of subchannels. As expected, the outage probability is increased when mobile users radiate more subchannels. We can also observe that as the link distance approaches and exceeds than 200 m, the outage probability reaches an unacceptable level. In other words, mobile users must locate in the vicinity of the BS to obtain high enough link quality when they require high speed transmissions.

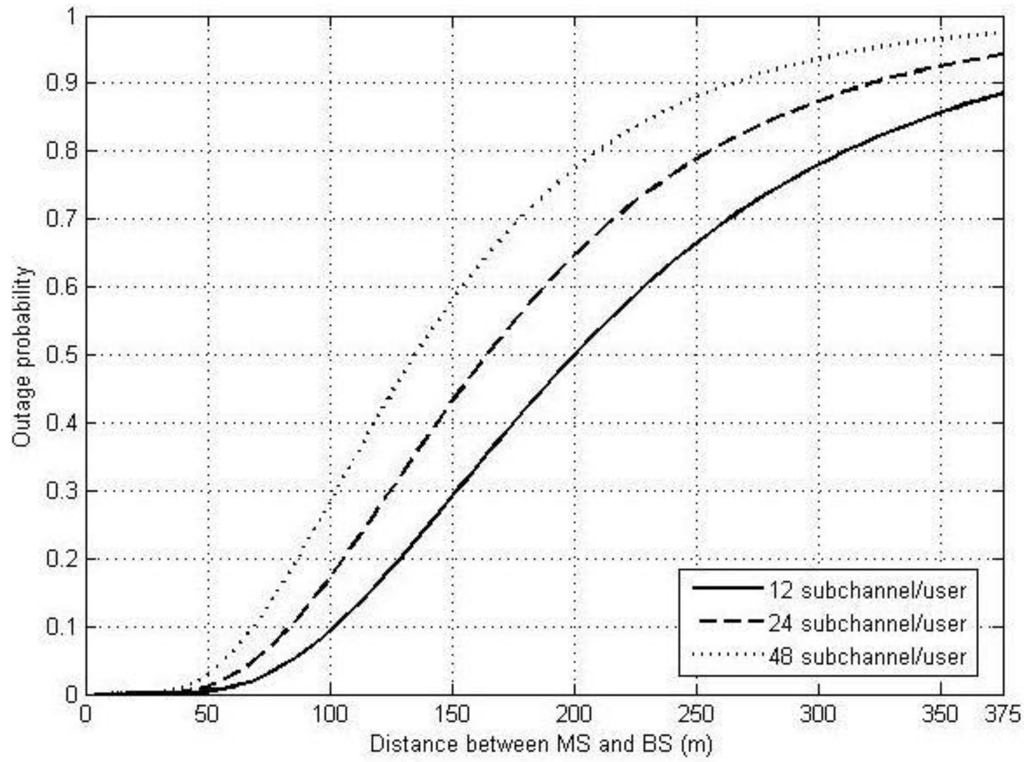

(a)

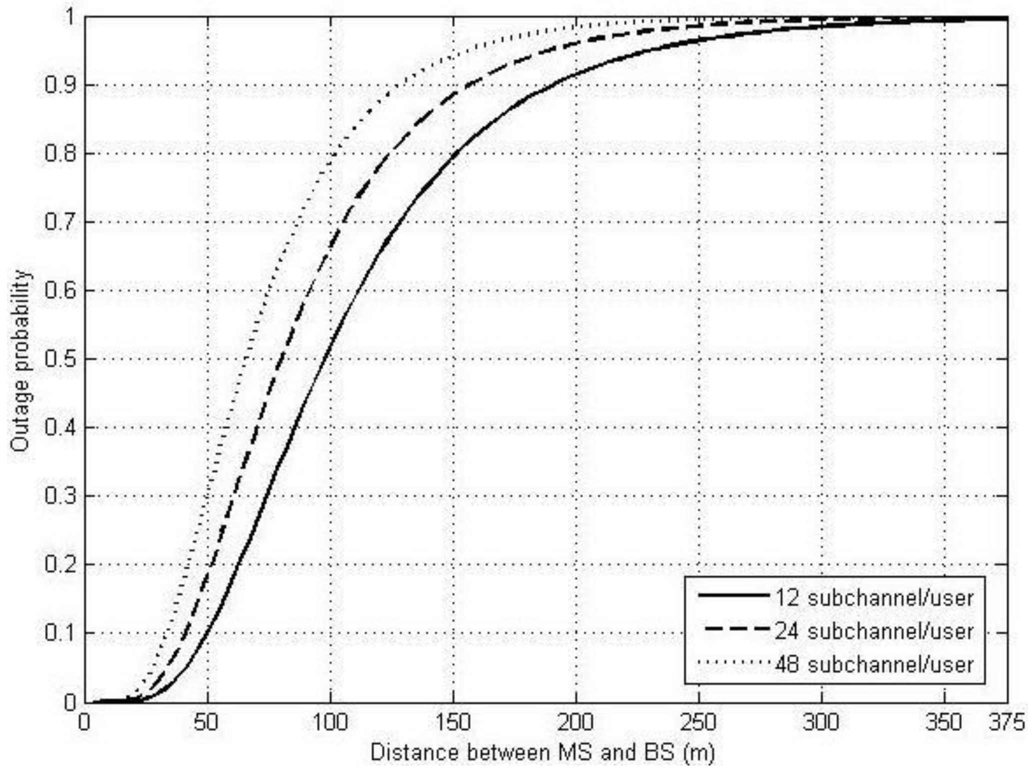

(b)

Figure 4.14 Influence of subchannel quantity assigned to mobile users on outage probability; (a) required SINR=6 dB, (b) required SINR=11.5 dB.

For uplink communications, the mobile device's power source, usually a DC battery, will significantly affect the communication link quality. In general, this kind of power supply cannot support long distance or high quality communications due to the limited power provisions. Figure 4.15 shows how a device's maximum power affects the service outage probability. We assign twelve subchannels to every user in this case. It can be found that when required SINR=6 dB, the cell coverage is about 105 m for the maximum power of 200 mW and will extend to about 165 m if the output power is increased to 1 W. Unfortunately, on the cell boundary (r=375m), all outage probabilities are greater than 0.5, even if the mobile device output power is up to 1W.

Next, we examine the relation between cell coverage and the number of subchannels used by mobile users. The maximum output power of mobile devices is set to 1 W in this case. Figure 4.16 presents the relation between cell coverage and the number of subchannels, taking the CCI effect into account. From the figure, we find that if mobile users need more subchannels or bandwidth — for example, six subchannels — their communication distances fall to 52 percent of the cell radius, 200 m. To obtain greater coverage, mobile users need to adopt a fewer subchannels or employ low spectral efficiency modulation schemes, such as QPSK, that require a lower SINR. For instance, if a mobile node uses one subchannel and QPSK modulation with 1/2 code rate (corresponding to SINR=6 dB), the communication distance can extend as long as 327 m, even if CCI exists. We can also find from the result that if mobile users need more than 12 subchannels, they should be located at a distance less than 160 m from their own BSs.

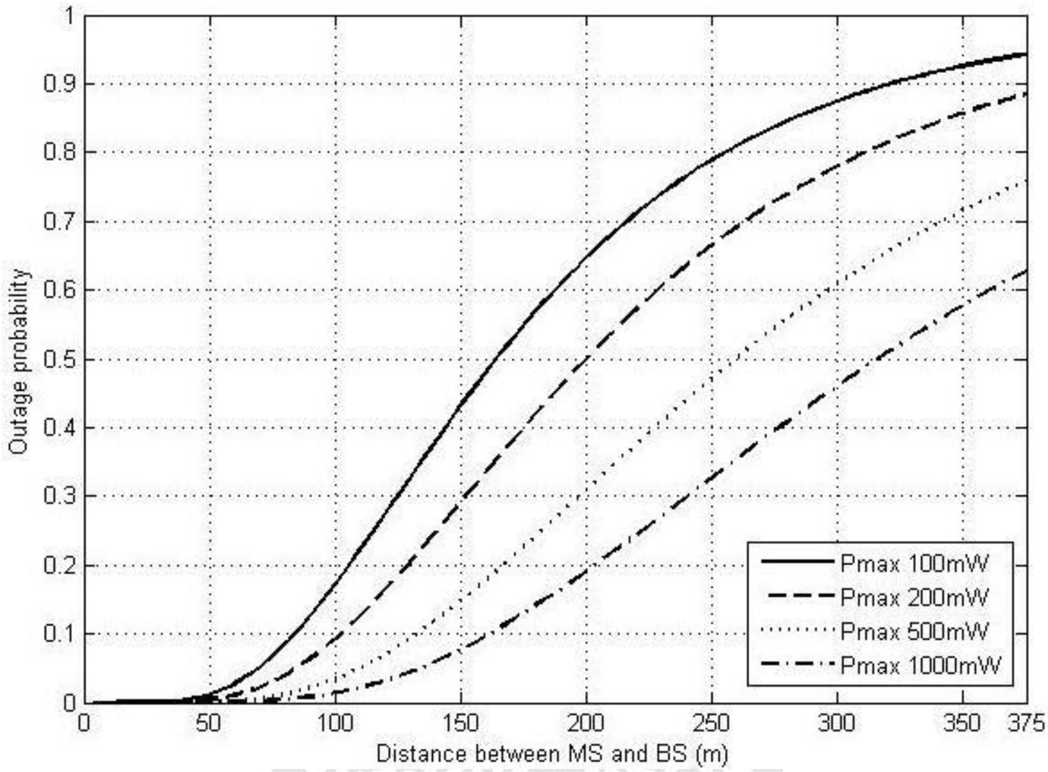

(a)

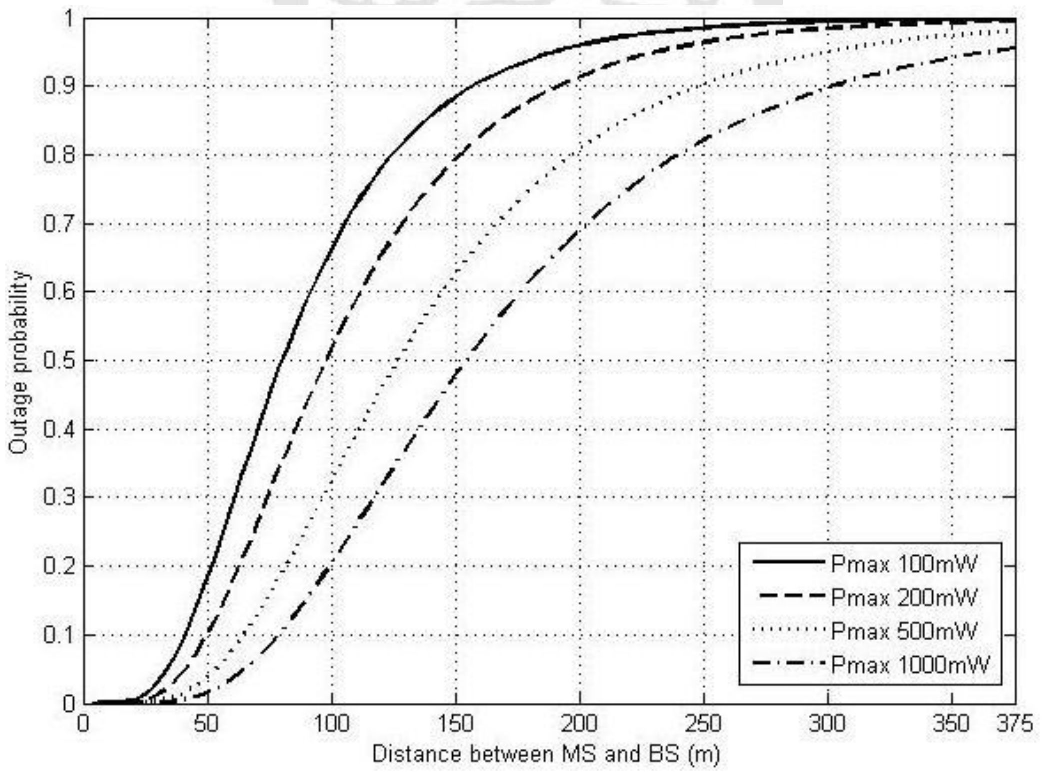

(b)

Figure 4.15 Influence of handset maximum power on outage probability; (a) required SINR=6 dB, (b) required SINR=11.5 dB.

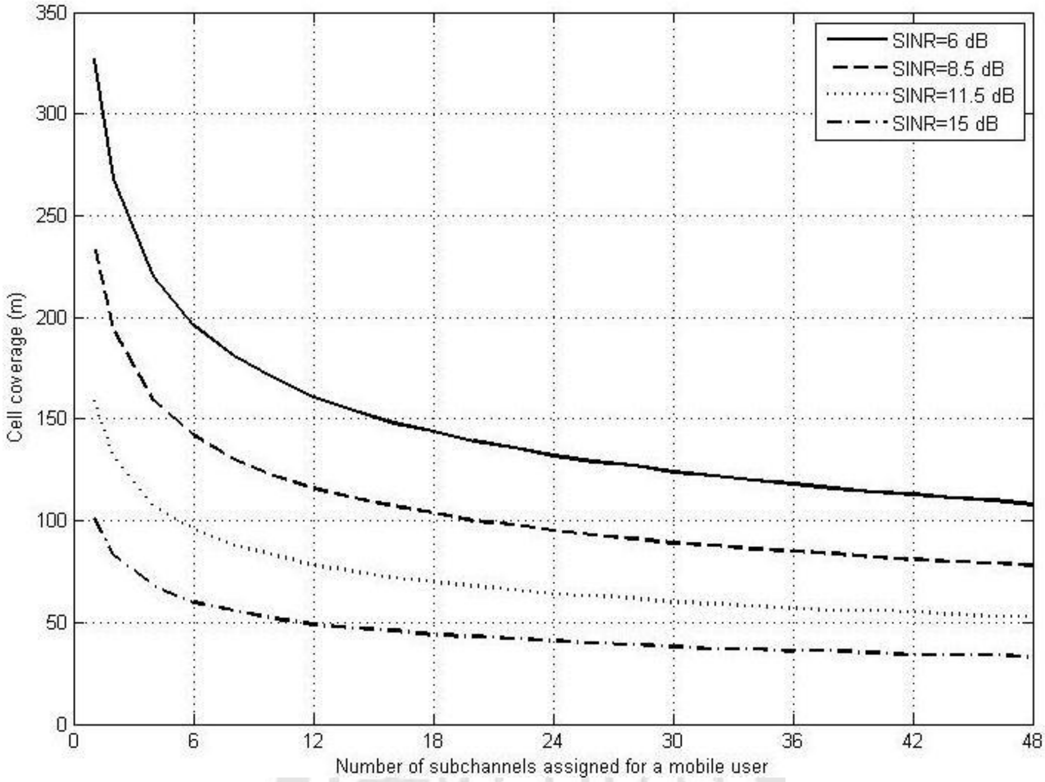

Figure 4.16 Relation between cell coverage and the number of subchannels.

Finally, we want to examine the reduction in cell coverage due to CCI. As shown in Figure 4.17, we find that for the case of SINR=11.5 dB and just one subchannel, the coverage radius can reach about 769 m without considering the CCI effect. To calculate the maximum service radius without CCI, we focus on the reference BS and ignore the cellular structure. Hence, the service radius could be greater than 375 m, which is the cell radius in the cellular configuration. If the CCI effect is taken into account, the service radius will significantly reduce to about 159 m. Similarly, consider the case of SINR=6 dB and 10 subchannels. The coverage radius will reduce to 170 m from 572 m due to the CCI effect. The above results reveal that the CCI can cause dramatic reduction in cell coverage. Considering the limitation of radio spectrum that can be used to deploy a wireless network, one of the possible solutions to mitigate the CCI impact is to increase the number of BSs, i.e., reduce the cell coverage. However, this solution can be cost-prohibitive, especially when the BS price is extremely high.

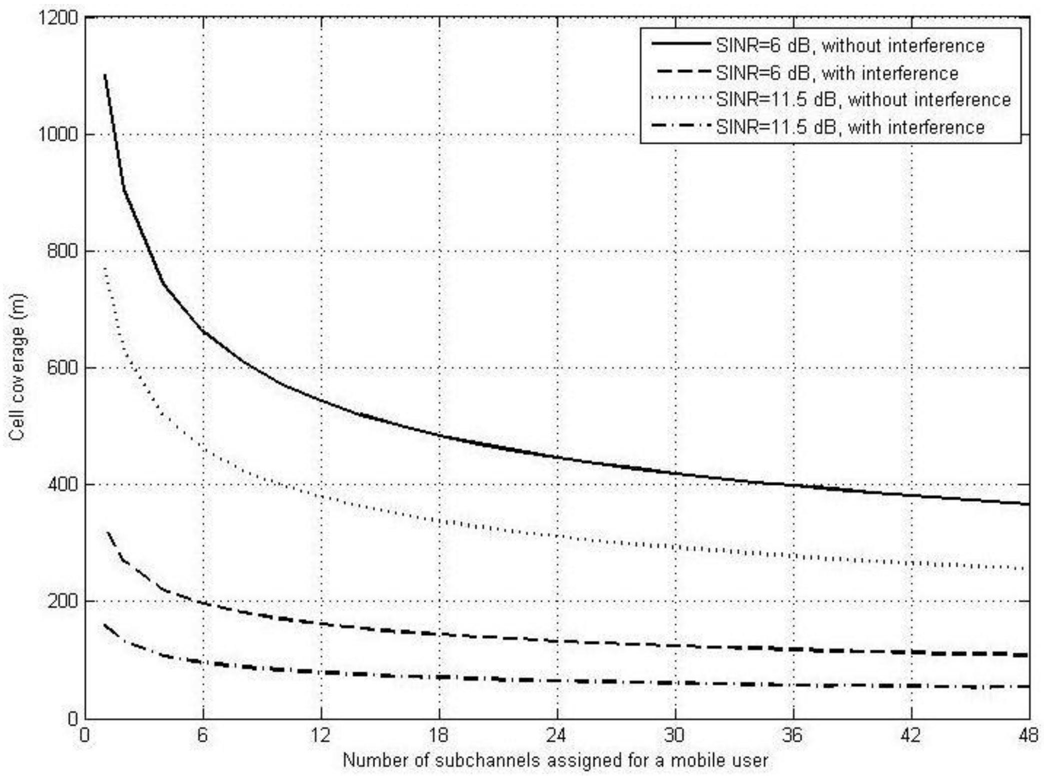

Figure 4.17 CCI impact on cell coverage with maximum output power of 1 W.

CHAPTER FIVE: CONCLUSIONS

This chapter consists of two sections. The conclusions drawn from this study are summarized in Section 5.1. Section 5.2 explains the limitations of this study and suggests areas for future research.

5.1 Conclusions

The first objective of this study is to develop a CCI analysis model, calculating the CCI power in the 4G wireless communication networks. This study develops a CCI estimation model for both downlink and uplink communication links. The frequency band, mobile user random locations, noise figure, propagation models, effect of shadow fading, equipment radiated power, and antenna pattern are considered in the CCI analysis models that we developed in this study.

The second objective of the study is to estimate the CCI impacts in 4G wireless communication networks on a system level. A radio network with a total of 19 BSs is employed in the study. The two-tier structure is based on the assumption that the radiated power would be too slight to detect over two times the base station coverage.

The CCI analysis in the downlink estimates the users' throughput based on the SINR. The impact of CCI is shown by the decrease of users' throughput. The lower throughput causes service failuressic when mobile users need a large amount of resources for high speed data transmissions.

Such as if a user accesses a video streaming service through the handset device. The media streaming quality can be acceptable using data rate 500 kbps for a 480 progressive scan (480p, 640×480) video or 800 kbps for a 720p (1280×720) video.

Users almost cannot watch the 720p video when CCI is taken into account. The 480p video streaming will lag when the system loading is greater than 0.5.

The analysis of the uplink estimates the reduction in cell coverage caused by CCI. The analysis model is based on the SINR requirement that the mobile user should radiate enough power to meet the BS minimum SINR requirement to ensure the communication link with the BS. The service outage probabilities are derived by taking handset output power limitations into consideration. The coverage reduction due to CCI can be evaluated by service outage probability.

The third objective of the study is to explore the effect and performance of CCI mitigation schemes. The FFR schemes are analyzed as the CCI mitigation schemes in the study. Two new FFR schemes are proposed to improve the spectral efficiency of 4G networks, particularly for cell-edge users. The two proposed schemes are based on typical PFR and SFR, respectively. Throughput performances that depend on the SINR received at mobile stations are employed to evaluate and compare the spectral efficiency of FFR schemes. The analysis compares the performance of FFR schemes deployed in urban and rural environments. Further, the influence of FFR schemes on cell-interior and cell-edge users discussed separately.

Under the limitation of radio spectrum, 4G operators must use frequency reuse schemes. Reusing the same frequency band frequently in the wireless communication system would bring co-channel interferences. Operators cannot ignore this situation and should search for solutions to mitigation the CCI impacts. According to our study, the FFR is an effective scheme to decrease the CCI influence.

5.2 Limitations and Suggestions for Future Research

There were several limitations to this study. First, to simplify the analysis, this study uses point-to-multipoint (PMP) architecture to model the CCI power. The relay architecture supported by both WiMAX and LTE is not included in this study. Second, the fading effect in this study takes only slow fading into consideration; fast fading is not addressed by our research.

This study uses two ICIC techniques, power control and FFR, to analyze how to the mitigate of CCI. Other common techniques are identified as ICIC approaches for wireless communication systems, such as spatial multiplexing, multi-user MIMO, opportunistic spectrum access, and organized beamforming. The comparison of different ICIC options can help 4G communication service providers to select suitable approaches to mitigate the CCI.

BIBLIOGRAPHY

[1] F. Wang, A. Ghosh, C. Sankaran, P. J. Fleming, F. Hsieh, and S. J. Benes, “Mobile WiMAX Systems: performance and evolution,” *IEEE Commun. Mag.*, pp. 41-49, Oct. 2008.

[2] IEEE std 802.16-2009, Part 16: Air interface for broadband wireless access systems, May 2009.

[3] IEEE std 802.16m-2011, Part 16: Air interface for broadband wireless access systems, May 2011.

[4] 3GPP TR 36.814, Further advancements for E-UTRA physical layer aspects (release 9), 2010.

[5] 3GPP TR 36.913, Requirements for further advancements for Evolved Universal Terrestrial Radio Access (release 10), 2011.

[6] H. Holma and A. Toskala, *LTE for UMTS OFDMA and SC-FDMA Based Radio Access*, Chippenham, UK, John Wiley & Son, 2009.

[7] A. Ghosh, P. Patasuk, B. Mondal, N. Mangalvedhe, and T. Thomas, “LTE-Advanced: Next-Generation Wireless Broadband Technology,” *IEEE Wireless Commun.*, vol.17, no. 3, pp.10-22, Jun. 2010.

[8] W.-T. Chen and J.-T. Lin, “Analysis of the Impacts of Uplink Co-Channel Interference on Cell Coverage in an IEEE 802.16m System,” *IEEE Trans. Veh. Technol.*, vol. 63, no. 5, pp. 2208-2215, Jun. 2014.

[9] H. Haas, V. D. Nguyen, P. Omiyi, N. Nedev, and G. Auer, “Interference aware medium access in cellular OFDMA/TDD networks,” in *Proc. IEEE ICC*, Jul. 2006, pp. 1778-1783.

[10] N. Himayat, S. Yalwar, A. Rao, and R. Soni, “Interference management for 4G cellular standards,” *IEEE Commun. Mag.*, pp. 86-92, Aug. 2010.

[11] G. Boudreau, J. Panicker, N. Guo, R. Chang, N. Wang, and S. Vrzic, “Interference coordination and cancellation for 4G networks,” *IEEE Commun. Mag.*, vol. 47, no. 4, pp. 74-81, Apr. 2009.

[12] S. J. Kao and H. L. Wang, “Dynamic Orthogonal Frequency Division Multiple Access resource management for downlink interference avoidance in two-tier

networks," *International Journal of Communication Systems 2013*; DOI: 10.1002/dac.2668.

[13] IST-4-027756 WINNER II deliverable D4.7.2, "Interference avoidance concepts," Jun. 2007.

[14] S. H. Ali and C. M. Leung, "Dynamic frequency allocation in fractional frequency reused OFDMA networks," *IEEE Trans. Wireless Commun.*, vol. 8, no. 8, pp.4286-4295, Aug. 2009.

[15] T. Novlan, J. G. Andrews, I. Sohn, R. K. Ganti, and A. Ghosh, "Comparison of fractional frequency reuse approaches in the OFDMA cellular downlink," *IEEE Global Telecomm. Conf. CLOBECOM*, Miami, Florida, USA, Dec. 2010, pp.1-5.

[16] 3GPP TR 36.913, Requirements for further advancements for Evolved Universal Terrestrial Radio Access (release 10), 2012.

[17] D. Astely, E. Dahlman, A. Furuskar, Y. Jading, M. Lindstrom, and S. Parkvall, "LTE: the evolution of mobile broadband," *IEEE Commun. Mag.*, vol. 47, no. 4, pp. 44–51, Apr. 2009.

[18] A. Kumar, Y. Liu, J. Sengupta, and Divya, "Evolution of mobile wireless communication networks: 1G to 4G." *International Journal of electronics & communication technology (IJECT)*, vol. 1, issue 1, pp. 68-72, Dec. 2010.

[19] M. Kottkamp, A. Roessler, and J. Schlienz, "LTE-Advanced technology introduction," Rohde & Schwarz, 1MA169_3E, 2012.

[20] M. Müller, "IEEE 802.16m technology introduction," Rohde & Schwarz, 1MA167_3E, 2010.

[21] S. Ahmadi, *Mobile WiMAX*, Academic Press, USA, 2011.

[22] T. Keller, L. Hanzo, "Adaptive multicarrier modulation: A convenient framework for time-frequency processing in wieless communications," in *Proc. of the IEEE*, vol. 8, issue 5, May 2000, pp. 611-640.

[23] M. Morelli, C.-C. J. Kuo, and M.-O. Pun, "Synchronization techniques for orthogonal frequency division multiple access (OFDMA): a tutorial review," in *Proc. Of the IEEE*, vol. 95, issue 7, Jul. 2007, pp. 1394-1427.

[24] R. V. Nee and R. Prasad, *OFDM for wireless multimedia communications*,

Boston: Artech House, 2000.

[25] S-E. Elayoubi, O. B. Haddada, and B. Fourestié, “Performance evaluation of frequency planning schemes in OFDMA-based networks,” *IEEE Trans. Wireless Commun.*, vol.7, no. 5, pp. 1623-1633, May 2008.

[26] A. E. Leu, B. L. Mark, and M. A. McHenry, “A framework for cognitive WiMAX with frequency agility,” in *Proc. of the IEEE*, vol. 97, no. 4, Apr. 2009, pp. 755-773.

[27] I. C. Wong and B. L. Evans, “Optimal downlink OFDMA resource allocation with linear complexity to maximize ergodic rates,” *IEEE Trans. Wireless Commun.*, vol. 7, no. 3, pp. 962-971, Mar. 2008.

[28] J. G. Andrews, A. Ghosh, and Muhamed, *Fundamentals of WiMAX: understanding broadband wireless networking*, Englewood-Cliffs, NJ, Prentice-Hall, 2007.

[29] Agilent Technologies, “Introducing LTE-Advanced,” 5990-6706EN, 2011.

[30] G. Fodor, A. Rácz, N. Reider, and A. Temesváry, “Architecture and Protocol Support for Radio Resource Management (RRM),” in *Long Term Evolution : 3GPP LTE* radio *and cellular technology*, B. Furht and S. A. Ahson, Eds. Taylor & Francis Group, 2009,ch. 4, p. 104.

[31] Jr. L. J. Cimini, “ Analysis and simulation of a digital mobile channel using orthogonal frequency division multiplexing,” *IEEE Trans. Commun.*, vol 33, no. 7, pp. 665-675, Jul. 1985.

[32] Y. G. El-Jaafreh, “Co-channel and adjacent channel interference calculations in cellular communications systems,” *Journal of King Saud University, engineering Sciences*, vol. 12, no. 1, pp. 153-168, 2000.

[33] W. T. Chen, “Adjacent channel interference in a macrocell/microcell WCDMA system,” Wireless *Communications and Mobile Computing*, vol. 9, no. 2, pp. 187-195, Feb. 2009.

[34] M. Coupechoux and J.-M. Kelif, “How to set the fractional power control compensation factor in LTE,” Sarnoff Symposium, 2011 34th IEEE, May 2011, pp.1-5.

[35] A. Simonssion and A. Furuskär, “Uplink power control in LTE-overview and

performance," *Vehicular Technology Conference*, Sep. 2008, pp.1-5.

[36] F. Hendessi, A. U. Sheikh, and R. M. Hafez, "Co-channel and adjacent channel interference in wireless cellular communications," *Wireless Personal Communications*, vol.12, pp. 239-253, Feb. 2000.

[37] Z. Xu, G. Y. Li, C. Yang, and X. Zhu, "Throughput and optimal threshold for FFR schemes in OFDMA cellular networks," *IEEE Trans. Wireless Commun.*, vol. 11, no. 8, pp. 2776-2785, Aug. 2012.

[38] M. Assaad, "Optimal fractional frequency reuse (FFR) in multicellular OFDMA system," *IEEE 68th Vehicular Technology Conf.* VCT 2008-Fall, Calgary, AB, Canada, Sep. 2008, pp. 1-5.

[39] IEEE 802.16 Broadband Wireless Access Working Group, "IEEE 802.16m Evaluation Methodology Document (EMD)," Jan. 2009.

[40] 3GPP TR 136.942, Radio frequency system scenarios (release 10), 2012.

[41] D. K. Kim and D. K. Sung, "Capacity estimation for a multicode CDMA system with SIR-based power control," *IEEE Trans. Veh., Technol.*, vol. 50, no. 3, pp. 701-710, May. 2001.

[42] T. D. Novlan, R. K. Ganti, A. Ghosh, and J. G. Andrews, "Analytical Evaluation of fractional frequency reuse for OFDMA cellular networks," *IEEE Trans. Wireless Commun.*, vol. 10, no. 12, pp. 4294-4305, Dec. 2011.

[43] M. Rahman and H. Yanikomeroglu, "Enhancing cell-edge performance: a downlink dynamic interference avoidance scheme with inter-cell coordination," *IEEE Trans. on Wireless Commun.*, vol. 9, no. 4, pp.1414-1425, Apr. 2010.

[44] IEEE 802.16 Broadband Wireless Access Working Group, "IEEE 802.16m System Description Document (SDD)," Sep. 2009.

LIST OF ACRONYMS

2G	Second Generation
3G	Third Generation
3GPP	3rd Generation Partnership Project
ACI	Adjacent-Channel Interference
BS	Base Station
CCI	Co-channel Interference
CDF	Cumulative Density Function
CDMA	Code Division Multiple Access
FDD	Frequency Division Duplexing
FFR	Fractional Frequency Reuse
GSM	Global System for Mobile Communications
ICIC	Inter-Cell Interference Coordination
IEEE	Institute of Electrical and Electronics Engineers
IMT-2000	International Mobile Telecommunications 2000
IMT-Advanced	International Mobile Telecommunications-Advanced
IN	Interfere Node
ITU	International Telecommunication Union
ITU-R	ITU Radiocommunication sector
LTE	Long Term Evolution
LTE-A	LTE-Advanced
MIMO	Multiple Input/Multiple Output
MU-MIMO	Multi User MIMO
MS	Mobile Subscribers

NF	Noise-Figure
OFDM	Orthogonal Frequency Division Multiplexing
OFDMA	Orthogonal Frequency Division Multiple Access
PFR	Partial Frequency Reuse
RB	Resource Block
RE	Resource Element
RN	Receive Node
SFR	Soft Frequency Reuse
SINR	Signal-to-Interference-plus-Noise Ratios
TDD	Time Division Duplexing
TN	Transmit Node
UMTS	Universal Mobile Telecommunications System
WCDMA	Wideband Code-Division Multiple Access
WiMAX	Worldwide Interoperability for Microwave Access